

Contents lists available at ScienceDirect

# Transportation Research Part B

journal homepage: www.elsevier.com/locate/trb





# Schedule negotiation with ADA paratransit riders under value of time uncertainty

Shijie Chen <sup>a</sup>, Md Hishamur Rahman <sup>b</sup>, Nikola Marković <sup>b</sup>, Muhammad Imran Younus Siddiqui <sup>c</sup>, Matthew Mohebbi <sup>c</sup>, Yanshuo Sun <sup>a,\*</sup>

- a Department of Industrial and Manufacturing Engineering, FAMU-FSU College of Engineering, Florida State University, Tallahassee, FL, US
- <sup>b</sup> Department of Civil and Environmental Engineering, University of Utah, Salt Lake City, UT, US

#### ARTICLE INFO

# Keywords: ADA paratransit Schedule negotiation Mixed integer nonlinear program Behavior uncertainty Case studies

#### ABSTRACT

When paratransit riders book their travels, operators have the flexibility to adjust the requested pickup time within a predetermined limit for efficiency purposes in accordance with the Americans with Disabilities Act (ADA) regulations. This practice, known as schedule negotiation, is widely adopted across the United States (U.S.). However, the existing paratransit literature lacks optimization methods to support decision-making in this context. To address this research gap, we propose a new mathematical formulation, enabling an operator to simultaneously determine how a new travel request can be accommodated and how incentives can be designed to maximize the operator's payoff (revenues minus total costs). In addition, to enhance the realism of behavioral modeling in the paratransit literature, we explicitly consider the privately held value of time information for riders, which results in probabilistic responses. Eventually, the formulation is a nonconvex mixed-integer nonlinear program (MINLP). We thus design a decomposition-based fix-and-optimize algorithm that ensures global optimality despite the nonconvexity. We validate and evaluate our proposed method through synthetic analyses and real-world case studies, which demonstrate substantial advantages of schedule negotiation in improving paratransit operational efficiency. We also highlight the efficiency of the proposed solution approach relative to a benchmark approach based on complete enumeration. The proposed optimization method is thus expected to advance the state of the practice in pickup time negotiation in paratransit and other related mobility services.

#### 1. Introduction

In compliance with the Americans with Disabilities Act (ADA) of 1990, all public transit operators in the United States (U.S.) provide specialized transportation services to individuals with physical impairments that prevent them from using conventional transit. These paratransit services are on-demand, which means the routes and schedules of the vehicles are optimized based on trip reservations made by paratransit riders in advance. While riders submit their travel requests, paratransit service providers can negotiate pickup times with eligible riders to yield operational benefits, such as reducing trip denials. ADA permits this as long as the schedule deviation is within one hour (FTA, 2020). Despite the wide adoption of this schedule negotiation practice by transit agencies throughout the U.S., including the Pioneer Valley Transit Authority (PVTA) in Massachusetts (PVTA, 2019) and Miami-Dade Transit

E-mail addresses: sc20hw@fsu.edu (S. Chen), u1400077@utah.edu (M.H. Rahman), nikola.markovic@utah.edu (N. Marković), myounus@itcurves.net (M.I.Y. Siddiqui), mmohebbi@itcurves.net (M. Mohebbi), y.sun@eng.famu.fsu.edu (Y. Sun).

c IT Curves, Gaithersburg, MD, US

<sup>\*</sup> Corresponding author.

in Florida (Miami-Dade County, 2015), among others, there is a lack of scholarly work on pickup time negotiation in paratransit. Given this significant research gap, the extent to which schedule negotiation can enhance service quality and operational efficiency in ADA paratransit and how such benefits can be achieved systematically remain unclear. Therefore, this study aims to propose an optimization method for ADA paratransit operators to conduct schedule negotiations with riders at the time of reservation.

While the optimization literature on the Dial-A-Ride Problem (DARP), which intends to optimize paratransit vehicle routes and schedules, is extensive, a significant research gap exists regarding the neglect of modeling DAR rider behavior in most DARP optimization studies. In other words, existing studies make vehicle routing and scheduling decisions solely based on the DAR operator's objective, without considering how riders might react to these decisions. Recent studies are beginning to move away from this restrictive assumption, opting to model riders as having choices rather than being merely captive to the service. For instance, Azadeh et al. (2022) optimized trip assortments (sets of trip alternatives associated with prices) and adopted utility functions to capture riders' characteristics. However, one underlying assumption in those studies is that a rider's utility function is fully specified and known to the operator, which may not hold in practice. For example, a rider's Value of Time (VoT) is not constant and varies with the travel period and purpose. At best, an operator can estimate the range or distribution for VoT, while the actual VoT is known only if a rider voluntarily discloses it. The issue arising from asymmetric information has been studied by Sun et al. (2020), nonetheless, in a very different study on public transit subsidization and regulation. The second research gap is that none of the DAR studies have fully considered the impact of private information held by ADA riders on DAR vehicle operations, in addition to the lack of scholarly work on pickup time negotiation in ADA paratransit.

It is essential for the operator to explicitly consider the private information about VoT of a rider in negotiating the pickup time with the rider. Offering too much incentive may negate the potential benefits of shifting a rider's schedule; an incentive deemed insufficient by a rider with uncertain VoT could likely result in the rejection of a suggested schedule deviation. Although the necessity is easy to observe, it is worth analyzing the implications of incorporating uncertain VoT for the formulation and solution of the schedule negotiation problem. The probabilistic response of a rider, arising from VoT uncertainty, implies the operator must maximize the expected payoff by considering both rider acceptance and denial. As shown in Sections 3 and 4, the optimization objective of the operator becomes nonlinear, and the optimization problem is no longer convex.

To fill the two aforementioned research gaps and address the methodological challenge arising from a rider's uncertain VoT, we present novel mathematical programming formulations and design a decomposition-based solution framework. Specifically, we first present a Mixed Integer Program (MIP) for the pickup time scheduling problem assuming full compliance of a rider, which is also called the Booking Confirmation Problem (BCP) in this paper. Then, we extend this formulation to the Negotiable BCP (N-BCP) by modeling the probabilistic response of a rider for confirmation. As the resulting optimization problem is a Mixed Integer Nonlinear Program (MINLP), which is later shown to be a nonconvex problem, we design a fix-and-optimize strategy to solve this problem optimally.

Our contribution is three-fold. First, this is the first known optimization study addressing the schedule negotiation between an ADA paratransit operator and its riders, considering the private information of a rider and thus modeling the partially compliant rider behavior. Second, we derive several important properties of the proposed N-BCP and propose a global optimization approach for solving the nonconvex problem optimally, based on a fix-and-optimize solution framework. Third, we conduct real-world case studies and derive managerial insights from the implementation of the proposed optimization method.

The remainder of this paper is organized as follows. Section 2 reviews the related literature and highlights the contributions of our study in light of the existing research. Section 3 defines the Booking Confirmation Problem (BCP) and introduces the negotiable BCP model. Section 4 explores structural properties and presents a solution approach. In Section 5, we present the computational results that illustrate the performance of our proposed framework. Finally, Section 6 concludes the paper and provides directions for future research.

#### 2. Literature review

# 2.1. Modeling of rider behavior in Dial-A-Ride problem

The Dial-A-Ride Problem (DARP) is a generalization of the extensively studied PDPTW (Pickup and Delivery Problem with Time Windows), as it is concerned with the fulfillment of a given set of travel requests with specific pickup and drop-off locations using a fleet of vehicles. The DARP is distinctive primarily because of its human dimension, which implies some level of service requirements (e.g., maximum ride time) (Bertsimas et al., 2019). Depending on whether trip requests are received beforehand, whether the relevant information is known with certainty, what problem features are considered, and what optimization objective is pursued, there are many DARP variants in the extensive DARP literature (Bongiovanni et al., 2019; Masmoudi et al., 2016; Luo et al., 2019; Braekers et al., 2014; Su et al., 2023; Diana and Dessouky, 2004). Various exact methods, heuristics, and metaheuristics have been developed to solve those DARP variants. For more systematic and comprehensive surveys, readers are directed to Molenbruch et al. (2017) and Ho et al. (2018). Here, we review two representative studies in detail.

Rist and Forbes (2021) is one of the latest studies on the static DARP, a predominant variant of the DARP, assuming that all trip requests are known in advance (Berbeglia et al., 2012). The new formulation proposed by Rist and Forbes (2021) was based on the notion of "restricted fragments", which were segments of a vehicle route satisfying certain conditions. Rist and Forbes (2021) developed effective methods to enumerate restricted fragments, proposed domination criteria to reduce the number of fragments, and defined new valid inequalities. The new formulation was solved by a branch and cut algorithm. Their computational results

indicated that nine benchmark instances were solved optimally for the first time and the computation time for other large instances was significantly reduced.

Unlike a static DARP, travel requests can be received in real-time in a dynamic DARP. When a request arrives, the operator tries to fulfill this request with the minimum incremental cost. Depending on the operational policy, the operator could reject a request, for instance, due to insufficient vehicle capacity (Coslovich et al., 2006). When a new travel request is accommodated, pre-planned or previously accepted requests cannot be reshuffled, because vehicles assigned to those requests could have been announced to riders (Wong et al., 2014). In this case, Wong et al. (2014) derived a counterintuitive conclusion about the effect of dynamism (quantified as the number of dynamic requests divided by the total number of requests) on the operational efficiency through simulation experiments. They found a "dilemma zone" of dynamism and claimed that when the degree of dynamism was around 70%, the transportation cost was the highest and the request acceptance rate was the lowest. In other words, a partial dynamic system has worse performance not only than a static system but also a fully dynamic system. The reason is that pre-planned requests can limit a DAR system's capability of accommodating dynamic requests.

The vast majority of studies on the DARP pay little attention to the choice behavior of riders, as it is implicitly assumed that the service provider makes all vehicle routing and scheduling decisions in a centralized manner, leaving riders no choice at all. This is partially true because, in any paratransit system, most riders are considered "captive" because they are not equipped with other travel options due to their disadvantaged economic conditions or physical barriers, among others. However, neglecting the paratransit demand characteristics and not properly managing the demand would likely lead to inefficient paratransit operations. Some good indicators of operational inefficiency are uneven vehicle loads, significant deadheading, and substantial service denials. For instance, if most riders request rides at a similar time, a temporal demand peak emerges, and so does the shortage of vehicles for dispatching. To remedy the potential demand-supply misalignment, the ADA allows a paratransit provider to negotiate pickup times with its riders. Many operators in practice also conduct schedule negotiations with riders in an *ad hoc* manner, primarily to reduce denials of services. Clearly, coordinating schedules among fellow riders could yield other operational benefits, such as reductions in vehicle idling, as shown later in this paper. Despite the potential of schedule negotiation, to the knowledge of the authors, no scholarly work is available for addressing this important issue.

Next, we provide detailed reviews of two studies that are particularly notable for their realistic modeling of rider behaviors in related on-demand services, even though the primary focus of those studies is not on schedule negotiation. In the mobility system considered by Dong et al. (2022), there exists a reserve travel mode, such as driving or taxi, in addition to the Demand-Responsive Transport (DRT) service. For each rider i, two utility functions  $\hat{V}_i$  and  $V_i$  are defined for the reserve mode and the DRT option, respectively. While the reserve mode's utility  $\hat{V}_i$  is fixed, the DRT's utility  $V_i$  depends on the operator's decisions, because both the travel time and schedule delay (e.g., waiting time at the pickup location) can be optimized by the operator. The operator seeks to ensure that the probability that the DRT's utility exceeds that of the reserve mode, namely  $\Delta U_i = \hat{V}_i - V_i \le 0$ , is at least p (a predefined probability). With such a chance constraint, the profit-driven operator selects only those riders who perceive the DRT significantly more favorably than the reserve mode for service. This is because Dong et al. (2022) assumed that riders with a higher DRT utility are more satisfied with DRT and less likely to cancel their reservations, thus positively contributing to high profits in the long run. This assumption is debatable, as accepting an outlier rider traveling in a remote area is hardly profitable, even though this outlier rider perceives DRT very favorably. Further, different fare structures were considered for revenue management at a strategic planning level. While this study considerably improves the behavior modeling of DRT riders with utility functions, riders remain to be captive, because the operator could select or reject a rider, while a rider is unable to deviate from the operator's decision in Dong et al. (2022).

Azadeh et al. (2022) considered a similar mobility system consisting of two options, i.e., dedicated and shared, however, in a dynamic setting. For each incoming request, the operator generates a range of personalized travel alternatives, which differ in modes and pickup delays. Those alternatives are further associated with different price levels, which were further used to create assortments. Then, the operator selects one assortment (a menu of alternatives associated with price levels) to maximize the expected profit by solving a mixed integer program, known as assortment optimization. A multinomial logit model is used to estimate the probability of choosing an alternative in an assortment. Unlike in Dong et al. (2022), a rider may select none of the alternatives included in the optimal assortment selected by the operator, i.e., reject the optimal assortment and choose an opt-out option. As expected, the computational performance of the developed approach by Azadeh et al. (2022) clearly depends on the number of alternatives considered and the price discretization level. For instance, when the price discretization level reduces to \$0.1, the assortment optimization problem could be intractable because of the unacceptable computation time. At present, the pickup time of a rider could be postponed by  $\Delta T$ ,  $2\Delta T$  or  $3\Delta T$ . It is much more challenging if the pickup delay is continuous, which implies an infinite number of alternatives.

While both Dong et al. (2022) and Azadeh et al. (2022) have significantly advanced the frontier in demand modeling in DRT or paratransit, they have some limitations. First, it is assumed that the utility function of a service mode for each rider can be specified, which is a practically challenging task. For instance, the value of time, which is essential in any utility function, depends on a rider's socio-economics and travel purpose. There is no straightforward way to obtain an accurate estimation. Thus, such information should be considered private and only a distribution or range could be available to the operator. The private information has major implications for the operator's decisions, as the operator can no longer force riders into certain choices selected by the operator. Moreover, considering the behavior uncertainty could result in a challenging nonlinear program, which makes this consideration nontrivial. Furthermore, although both studies mentioned "dial-a-ride", their considered services do not resemble the so-called ADA paratransit service in the U.S. context. For example, ADA paratransit riders cannot drive or have other private travel options. ADA paratransit fares are highly regulated and cannot exceed twice as much as a comparable transit trip's fare. Additionally, both studies use New York City taxi trip data to generate their test cases, while the characteristics of the taxi trip could differ significantly from the travel patterns of ADA riders.

#### 2.2. Demand management in relevant delivery problems

Although the literature on customer behavior modeling in the ADA paratransit context is quite limited, customer choice modeling has been extensively studied in some freight transportation problems where operational efficiency hinges on customer preferences and choices (McGill and Van Ryzin, 1999; Zhang and Adelman, 2009; Strauss et al., 2018). For instance, Attended Home Delivery (AHD) requires a customer to be present when a delivery is made (Agatz et al., 2011). Therefore, a delivery company must agree on a slot with a customer (Ehmke and Campbell, 2014). As most customers may prefer certain slots during rush hours, such as weekday evenings, the delivery company needs to decide how to offer delivery slots and optimize pricing considering the effect on customer choices. A good number of studies have focused on AHD demand management, which can be divided into two groups based on the type of a company's decision, namely slot pricing and availability control (Fleckenstein et al., 2023).

In price-based control, delivery slots are associated with different incentives or surcharges in order to influence customer choices favorably. For instance, in an AHD slot pricing study, Klein et al. (2019) optimized the price of each delivery slot for each ZIP code to maximize the total profit. In modeling customer choice behavior, they assumed that all customers in a segment had the same preference ranking and would choose the time slot price point combination (TPC) with the highest ranking. In other words, it was assumed that the TPC choice by a customer could be anticipated by the delivery company with certainty. Unlike Klein et al. (2019) where offline orders were considered, Vinsensius et al. (2020) considered a dynamic problem where orders arrive over time. Vinsensius et al. (2020) adopted a simplified assumption about the probability of selection. Basically, the probability that a customer will choose a slot is a linear function of the offered incentive.

The other type of demand management strategy, namely availability control, has been studied by Mackert (2019), among others. Mackert (2019) studied a dynamic time slot allocation problem without pricing, where a time slot should be offered only when the generated profit from doing so exceeds the opportunity cost, which is difficult to estimate. The opportunity cost arises because certain future orders cannot be served if scarce resources (delivery capacity) are committed to a current order. Therefore, Mackert (2019) developed various approaches for estimating such an opportunity cost. For more relevant reviews, readers can refer to Waßmuth et al. (2023).

Based on the aforementioned reviews, it is evident that the literature concerning the integration of demand management and delivery optimization in the field of AHD has been extensive. However, it should be noted that while the developed methods are applicable within the context of AHD, their direct transferability to ADA paratransit is limited due to several fundamental differences between these two domains. For instance, as agreed by Klein et al. (2019), the AHD literature generally does not address the explicit optimization of the individual route due to the intractability. Instead, AHD-associated studies focus on the time slot perspective by approximating the routing cost (Klein et al., 2019; Agatz et al., 2011). Moreover, paratransit fare is highly regulated, while the delivery fee can be freely designed in AHD. The underlying vehicle routing problem in AHD is also quite different from the pickup and delivery problem in paratransit due to the human dimension.

#### 2.3. Summary

Despite decades of extensive research on the Dial-A-Ride Problem, the level of modeling realism for riders has remained relatively low in the literature, mainly because riders are often assumed to be captive. Surprisingly, the scholarly literature has largely overlooked the pickup time negotiation aspect in paratransit, despite its wide implementation in practice and support by federal law. In light of the innovative demand management strategies applied to other delivery problems, this paper thus proposes a novel method for schedule negotiation, by realistically modeling the choice behaviors of paratransit riders with private information.

#### 3. Problem statement

#### 3.1. Overall decision-making problem

In the ADA paratransit system considered here, riders book their trips dynamically. The service provider cannot anticipate such bookings as the detailed information contained in a booking, such as an origin, destination, and requested pickup time, is known only after a booking is received. At the present time  $\tau$ , the set of trip bookings  $B_{\tau}$  received before  $\tau$  has been confirmed, which means that the rider involved in each booking  $b \in B_{\tau}$  has been covered by a vehicle route  $w \in W_{\tau}$  with all relevant constraints satisfied, such as the pickup time window requirement and ride time limit. The routes in set  $W_{\tau}$  are also known as existing routes. For the next trip booking i received at time  $h_i$ , the requested pickup time window is denoted as  $[e_i, l_i]$ , where  $e_i$  and  $l_i$  are the earliest and latest pickup times, respectively. As advance booking is required by regulations, we must have  $e_i \ge h_i + \Omega$ , where  $\Omega$  is the minimum advance booking time, e.g., two hours. To ensure timely feedback, shortly after receiving the reservation i, the service provider must complete the confirmation by modifying an existing vehicle route or creating a new vehicle route, which is called the *Booking Confirmation Problem* (BCP) in this study and is illustrated in Fig. 1.

In the BCP, the provider seeks to maximize its payoff (i.e., total revenue minus total cost) after booking i is confirmed. As the provider is not allowed to reject a request, maximizing the payoff is equivalent to minimizing the total service cost. As all existing bookings in  $B_{\tau}$  were previously confirmed, it is required that the relative pickup and drop-off sequence for those riders covered by an existing route can no longer be changed and no rider-specified constraints can be violated, either. After solving the BCP for booking i and notifying the rider, the provider awaits the next booking i + 1, which triggers a new receiving-confirming cycle, until the end of a booking acceptance period.

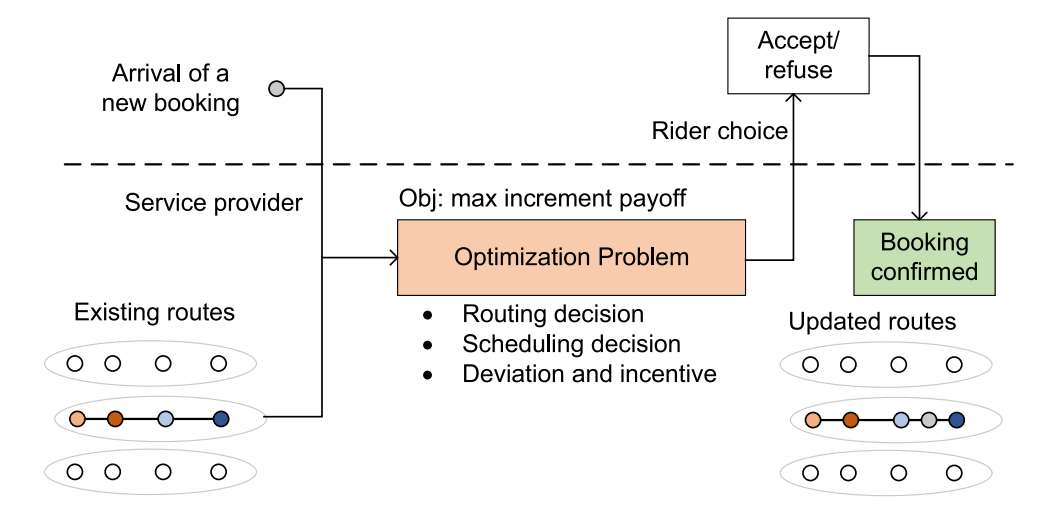


Fig. 1. Booking arrival and confirmation process.

Depending on how well the new rider's schedule aligns with the existing riders and whether the rider's schedule is flexible, the provider may confirm a new rider with a certain schedule deviation. More specifically, the requested pickup time window by the rider could be shifted earlier or later by the provider. If the provider accommodates a rider with schedule deviations, an incentive proportional to the magnitude of deviation is offered to the rider. There are two alternative assumptions on the behavioral response of the rider: full compliance vs. partial compliance. In the former case, a rider accepts any trip arrangement (including the amount of incentive) returned by the provider once all specified constraints are satisfied (e.g., maximum ride time). In other words, no negotiations are involved between the provider and rider. In the latter case, an autonomous rider with private information could accept the proposed change and the associated incentive or insist that the original schedule be followed. Essentially, the provider seeks to incentivize a rider to alter the individual's schedule for a system-wide efficiency gain. However, a rider may decline a schedule deviation proposed by the provider. After a travel request is confirmed, the underlying rider will not be involved in further negotiations, thus avoiding repeated travel schedule adjustments.

In Section 3.2, we study a simplified BCP by assuming the full compliance of a rider. In Section 3.3, we present an extended problem by modeling the probabilistic response of a rider. In Section 3.4, we seek to address the infeasibility issue arising from accommodating a new rider with existing routes.

# 3.2. Booking Confirmation Problem (BCP)

For a given existing route w and a new rider i, we need to find where to insert the pickup and drop-off nodes (denoted as  $o_i$  and  $d_i$ , respectively) into route w, namely routing decision, and further determine when each node of a route is visited by the underlying vehicle, namely scheduling decision. As illustrated in Fig. 2, route w covers two confirmed bookings, namely 1 and 2, and is visualized by red arcs. The relative pickup and drop-off sequence  $[o, o_1, o_2, d_1, d_2, d]$  has been confirmed and cannot be modified, although two new nodes  $o_3$  and  $d_3$  can be further included in route w. Possible new arcs for selection are added as follows: create a directed path connecting o,  $o_3$ ,  $d_3$ , and d sequentially; create a bidirected arc between the new pickup node  $o_3$  and each existing pickup or drop-off node (i.e., each node in  $\{o_1, o_2, d_1, d_2\}$ ); similarly, create a bidirected arc between the new drop-off node  $d_3$  and each node in  $\{o_1, o_2, d_1, d_2\}$ . The set of all directed arcs is denoted as d. As shown in Fig. 2, no direct arcs between existing pickup and drop-off nodes, such as between  $o_1$  and o, are included in o, because the relative pickup and drop-off sequence is modified otherwise.

The pickup time window  $[e_i, l_i]$  requested by a rider may be shifted to  $[e_i - b, l_i - b]$  or  $[e_i + b, l_i + b]$ , where b represents a deviation, defined as a non-negative continuous variable. To compensate for the schedule deviation, the provider offers an incentive of vb, where the compensation rate v translates time to money.

The essence of the BCP is to construct a vehicle route and schedule from depot o to depot d ensuring that both  $o_i$  and  $d_i$  are further covered, subject to applicable constraints. With the additional notation in Table 1, we present a mixed integer programming formulation for the BCP.

(BCP) 
$$\max_{\{x_{ij}, z, s_i, u_i, b\}} \Delta \pi_1^w = \sum_{i \in P} \rho_i - \left( \beta_1 \sum_{(i,j) \in A} c_{ij} x_{ij} + \beta_2 \sum_{(i,j) \in A} t_{ij} x_{ij} + \beta_3 \sum_{i \in P} s_i \right) - vb - \eta_w - \pi_w$$
 (1)

$$s.t. \sum_{i \in P} x_{oi} = 1 \tag{2}$$

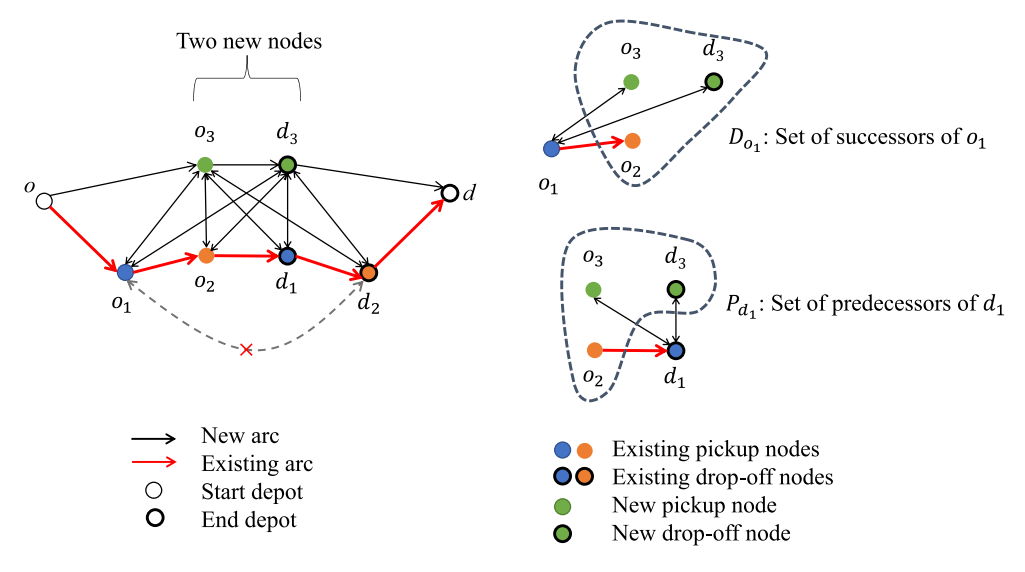


Fig. 2. Network for incorporating a new rider into an existing route. (For interpretation of the references to color in this figure legend, the reader is referred to the web version of this article.)

Table 1 Notation for the BCP.

Indices and sets	
P	Set of pickup nodes
D	Set of drop-off nodes
V	Set of all nodes, namely $V = \{o, d\} \cup P \cup D$
i, j	Node, $i, j \in V$
î	Rider for confirmation
$P_i$	Set of predecessors of node i
$D_i$	Set of successors of node <i>i</i>
A	Set of all arcs $(i, j)$
В	Set of all tuples in the format of (pickup, drop-off)
Parameters	
$ ho_i$	Revenue from serving rider $i$ , $\forall i \in P$
$\epsilon_i$	Service duration at node $i$ , $\forall i \in V$
$c_{ij}$	Travel distance from $i$ to $j$ , $\forall (i, j) \in A$
$t_{ij}$	Travel time from $i$ to $j$ , $\forall (i, j) \in A$
$R_{ij}$	Maximum ride time from pickup node i to drop-off node $j$ , $\forall (i,j) \in B$
$\bar{s_i}$	Upper bound on $s_i$ , $\forall i \in P$
$\beta_1, \beta_2, \beta_3$	Cost coefficients for driving distance, driving time, and idling time, respectively
$\pi_w$	Payoff of an existing route $w$ before accommodating a new rider
$\eta_w$	Total incentives claimed by existing riders in route $w$
M	A large constant
Decision variables	
$x_{ij}$	$x_{ij} = 1$ if arc $(i, j)$ is traversed by the vehicle; 0, otherwise
z	z = 1 if the pickup time window is shifted to the right; 0, otherwise
$S_i$	Vehicle idling time at node i
$u_i$	Vehicle arrival time at node i
b	Magnitude of deviation

$$\sum_{i \in D} x_{id} = 1 \tag{3}$$

$$\sum_{i \in D} x_{id} = 1$$

$$\sum_{j \in D_i} x_{ij} = 1, \quad \forall i \in P \cup D$$

$$\sum_{j \in P_i} x_{ji} = 1, \quad \forall i \in P \cup D$$
(5)

$$\sum_{i \in P_i} x_{ji} = 1, \quad \forall i \in P \cup D \tag{5}$$

$$u_i + s_i + \epsilon_i + t_{ij} - (1 - x_{ij}) M \le u_j, \quad \forall (i, j) \in A$$
 (6)

$$u_{j} \le u_{i} + s_{i} + \epsilon_{i} + t_{ij} + \left(1 - x_{ij}\right)M, \quad \forall (i, j) \in A$$

$$(7)$$

$$u_j - (u_i + s_i + \epsilon_i) \le R_{ij}, \quad \forall (i, j) \in B$$
 (8)

$$e_i \le u_i + s_i \le l_i, \quad \forall i \in P \setminus \{\hat{i}\}$$

$$e_i^2 - b - M(1-z) \le u_i^2 + s_i^2 \le l_i^2 - b + M(1-z)$$
 (10)

$$e_{\hat{i}} + b - Mz \le u_{\hat{i}} + s_{\hat{i}} \le l_{\hat{i}} + b + Mz \tag{11}$$

$$0 \le s_i \le \bar{s}_i, \quad \forall i \in P \tag{12}$$

$$s_j = 0, \quad \forall j \in D \tag{13}$$

$$0 \le b \le \bar{b} \tag{14}$$

$$z \in \{0, 1\} \tag{15}$$

$$x_{ij} \in \{0, 1\}, \quad \forall (i, j) \in A$$
 (16)

The objective Eq. (1) is to maximize the incremental payoff after confirming a new booking, which is computed as total revenue  $\sum_{i \in P} \rho_i$  minus total cost minus incentives minus the existing payoff  $\pi_w$ . The total cost is a weighted sum of driving distance  $\sum_{(i,j)\in A} c_{ij} x_{ij}$ , driving time  $\sum_{(i,j)\in A} t_{ij} x_{ij}$ , and idling time  $\sum_{i\in P} s_i$ .  $\eta_w$  represents the total incentives claimed by the existing riders covered by route w before a new rider  $\hat{i}$  is accommodated. Eq. (2) requires the vehicle to visit a pickup node immediately after leaving depot o. The vehicle must return to depot d from a drop-off node, not a pickup node, as enforced by Eq. (3). Eq. (4) means for each pickup or drop-off node, the vehicle must leave from it once; Eq. (5) means the vehicle must arrive at it once. Eqs. (6) and (7) ensure that if arc (i, j) is traversed, the arrival time at node j is exactly the sum of the arrival time at node i, idle time at node i, service duration at node i, and direct travel time from i to j. As the total service duration is constant for a given set of riders P, it is not included in the optimization objective. Eq. (8) states that the actual travel time from i to j for rider i must be less than  $R_{ij}$ . We further note that while sets A and B have common elements, B is not necessarily a subset of A, because the existing route has been confirmed and its pickup and drop-off sequence cannot be modified. For instance,  $(o_1, d_1)$  is in set B while it is not in set A in the example network shown in Fig. 2, as node  $o_2$  precedes  $d_1$  in the existing route. Eq. (8) also ensures that each rider is picked up before being dropped off. For all existing riders, Eq. (9) ensure that their pickup time windows are honored. Depending on the value of a binary variable z, the pickup time window of the new rider  $\hat{i}$  under negotiation can be shifted to the left (described by Eq. (10)) or right (described by Eq. (11)). Eq. (12) defines the range for  $s_i$  at pickup node i; Eq. (13) prevents vehicle idling at drop-off location j. Eq. (14) defines the range for b. Finally, Eqs. (15) and (16) define z and  $x_{ij}$  as binary variables, respectively. Note that DAR vehicle capacity constraints are mostly superfluous in practice because the maximum vehicle occupancy is below five while a DAR vehicle typically accommodates seven or more. When much smaller vehicles are employed, such vehicle capacity constraints can be added.

When b is fixed at 0 by setting  $\bar{b}$  to 0, the new rider must be accommodated without any schedule deviations. In this case, the maximum incremental payoff that can be achieved for route w is denoted as  $\Delta \pi_0^w$ , where subscript "0" means schedule deviations are absent. When the zero deviation requirement is relaxed, i.e.,  $\bar{b}$  is strictly positive,  $\Delta \pi_0^w$  serves as a lower bound on the maximum incremental payoff that is achievable, i.e.,  $\Delta \pi_1^w \geq \Delta \pi_0^w$ . This is intuitive because lifting a hard constraint cannot yield worse results.

#### 3.3. Negotiable Booking Confirmation Problem (N-BCP)

In Section 3.2, it is assumed that a rider always accepts a deviation of b for an incentive of vb, which is not realistic. Next, we extend the BCP formulation by modeling a rider's probabilistic acceptance of a schedule deviation and incentive, which is determined by a rider's private information, specifically the individual value of time (VoT). To decide whether to accept the deviation and incentive, a rider compares the compensation rate chosen by the provider v with his/her VoT. If v is smaller than the VoT, the rider declines the proposed deviation due to insufficient incentives. While the provider cannot know the true VoT, the probability for a rider to accept the deviation is  $\mathbb{P}(\text{VoT} \leq v)$ , which is  $\Phi\left(\frac{v-\mu}{\sigma}\right)$  when the rider's uncertain VoT follows a normal distribution with a mean of  $\mu$  and a standard deviation of  $\sigma$ . Here,  $\Phi\left(\cdot\right)$  is the cumulative distribution function of a standard normal distribution. If a proposed schedule deviation is accepted by the rider, the incremental payoff of route w after confirming a new booking is  $\Delta \pi_1^w$  given in Eq. (1). In case of a denial, another payoff, namely  $\Delta \pi_0^w$ , is achieved and the request is accommodated with no schedule deviations.

Anticipating the probabilistic response of a rider, the provider seeks to solve a negotiable BCP problem. The optimization objective is to maximize the expected payoff, namely

(N-BCP) 
$$\max_{\left\{x_{ij}, z, s_{i}, u_{i}, v, b\right\}} \mathbb{E}\left(\Delta \pi^{w}\right) = \boldsymbol{\varPhi}\left(\frac{v - \mu}{\sigma}\right) \Delta \pi_{1}^{w} + \left(1 - \boldsymbol{\varPhi}\left(\frac{v - \mu}{\sigma}\right)\right) \Delta \pi_{0}^{w},$$
 (17)

subject to all constraints in the BCP, i.e., Eqs. (2)-(16), and the following constraint:

$$v_{\min} \le v \le \bar{v},\tag{18}$$

where  $v_{\min}$  and  $\bar{v}$  are the lower and upper bound of v, respectively. Note that in the N-BCP, v becomes a variable to be optimized by the operator. When v increases, the acceptance probability  $\Phi\left(\frac{v-\mu}{\sigma}\right)$  increases monotonically; however,  $\Delta\pi_1^w$ , which is a function of v, might decrease if all other variables are held constant. Clearly,  $\Phi\left(\frac{v-\mu}{\sigma}\right)\Delta\pi_1^w$  is a nonlinear function of v.

The optimization objective Eq. (17) can be rearranged as

$$\mathbb{E}\left(\Delta \pi^{w}\right) = \Phi\left(\frac{v - \mu}{\sigma}\right) \left(\Delta \pi_{1}^{w} - \Delta \pi_{0}^{w}\right) + \Delta \pi_{0}^{w}.\tag{19}$$

Recall from Section 3.2 that  $\Delta \pi_1^w \geq \Delta \pi_0^w$ , there two cases, namely (1)  $\Delta \pi_1^w = \Delta \pi_0^w$  and (2)  $\Delta \pi_1^w > \Delta \pi_0^w$ . As  $\Delta \pi_0^w$  is constant in the N-BCP, we are only interested in case (2)  $\Delta \pi_1^w - \Delta \pi_0^w > 0$ , because in case (1), engaging in negotiations is futile. In case (1)  $\Delta \pi_1^w = \Delta \pi_0^w$ , the optimum schedule deviation b is zero, and the value of v is irrelevant.

To check whether  $\Delta \pi_1^w$  is strictly larger than  $\Delta \pi_0^w$  for route w, we can solve the N-BCP problem by setting the upper bound on b, i.e.,  $\bar{b}$ , to the ADA policy limit (60 min), and at the same time replacing the objective of the N-BCP (i.e., Eq. (17)) with Eq. (1). In other words, we solve the following problem:

$$\max_{\{x_{ij}, z, s_i, u_i, v, b\}} \Delta \pi_1^w = \sum_{i \in P} \rho_i - \left( \beta_1 \sum_{(i, i) \in A} c_{ij} x_{ij} + \beta_2 \sum_{(i, i) \in A} t_{ij} x_{ij} + \beta_3 \sum_{i \in P} s_i \right) - vb - \eta_w - \pi_w, \tag{20}$$

subject to Eqs. (2) to (16), and Eq. (18).

To solve the above problem, we actually only need to solve the BCP while fixing v at  $v_{\min}$ . This is because v is not part of Constraints (2) to (16) and the objective  $\Delta \pi_1^w$  is monotonically decreasing in v over range  $\left[v_{\min}, \bar{v}\right]$ , as proved in Section 4.1. Then, fixing v reduces the above problem to BCP.

If the resulting objective  $\Delta\pi_1^w$  is strictly larger than  $\Delta\pi_0^w$  for route w, we can solve the N-BCP for route w and obtain the maximum expected incremental payoff. It should be noted that when the N-BCP is solved optimally, we have  $\Phi\left(\frac{v-\mu}{\sigma}\right) > \left(1-\Phi\left(\frac{v-\mu}{\sigma}\right)\right)$  because  $\Delta\pi_1^w > \Delta\pi_0^w$ . This further means the lower bound on v, namely  $v_{\min}$ , should be tightened as  $\mu$ , which leads to  $\Phi\left(\frac{v-\mu}{\sigma}\right) > 0.5$ . Tightening the lower bound for v facilitates the concavity analysis in Section 4.2.1.

We then use  $\mathbb{E}\Delta\pi^{\max}$  to denote  $\operatorname{Max}_w \mathbb{E}(\Delta\pi^w)$ . It is not difficult to find  $\mathbb{E}\Delta\pi^{\max} \geq \operatorname{Max}_w \Delta\pi_0^w$ , because  $\mathbb{E}\Delta\pi^w \geq \Delta\pi_0^w$  for any route w. This means negotiating with a rider with uncertain VoT for schedule deviations would not yield an inferior result when the expected payoff is evaluated.

#### 3.4. A revised N-BCP addressing route infeasibility

In Section 3.2, it is assumed that it is always feasible for each route w to accommodate a new rider i. In case of an infeasible route,  $\Delta \pi_0^w$  is unavailable because rider i cannot be served by modifying route w. Then, this infeasible route is removed from consideration because the optimization objective of the N-BCP (namely Eq. (17)) cannot be constructed. Actually, a route that is infeasible under zero deviations may likely become feasible when schedule deviations are allowed. Turning an infeasible route into a feasible one could generate significant payoff improvements at the expense of minimal incentives. Therefore, we present a new modeling framework that addresses the infeasibility issue.

For each existing route w and a new rider, we first solve the BCP with  $\bar{b}=0$  and obtain  $\Delta\pi_0^w$ . If a rider cannot be feasibly accommodated by any existing routes when  $\bar{b}=0$ , a new route is created. Then, we denote  $\Delta\pi_0^{\max}=\max_w \Delta\pi_0^w$ . Then, the optimization objective of the N-BCP, namely Eq. (19), can be revised as follows:

$$\mathbb{E}\left(\Delta\pi^{w}\right) = \Phi\left(\frac{v-\mu}{\sigma}\right)\left(\Delta\pi_{1}^{w} - \Delta\pi_{0}^{\max}\right) + \Delta\pi_{0}^{\max}.\tag{21}$$

This is because regardless of which proposed route w with schedule deviations is declined by a rider, the provider can achieve  $\Delta \pi_0^{\max}$ , which is obtained when  $\bar{b} = 0$ . Next, the revised N-BCP can be solved for each route w, which yields  $\mathbb{E} \Delta \pi^{\max} = \max_w \mathbb{E} (\Delta \pi^w)$ .

The clear advantage of the revised N-BCP formulation is that those infeasible routes under zero deviations are further considered in solving the negotiation problem.

# 4. Solution approach

The N-BCP formulation is a nonconvex mixed integer nonlinear program (to be shown later in this section), which cannot be solved by any off-the-shelf solvers. A custom fix-and-optimize solution approach is thus proposed. For readability, the structure of this section is described as follows. In Section 4.1, we analytically derive some properties of the BCP, a Mixed Integer Program (MIP), when customers fully comply with any compensation rate v and discrete variables are fixed. Section 4.2 proves the concavity of the N-BCP's objective for fixed values of discrete variables and presents how to solve the N-BCP optimally utilizing the concavity. Section 4.3 describes how to identify promising values of discrete variables. Finally, we state how to jointly optimize discrete and continuous variables, which ensures global optimum.

#### 4.1. Solving the BCP assuming full compliance for fixed discrete variables

We investigate how to address the BCP problem, namely Eqs. (1) to (16), where a rider willingly accepts all schedule deviations regardless of the magnitude of v. In BCP, v is a known input/parameter;  $x_{ij}$  and z are discrete variables; the other variables are continuous, namely  $s_i$ ,  $u_i$ , and b.

**Proposition 1.** When the values of discrete variables  $x_{ij}$  and z are fixed in the BCP, the values of all other continuous variables, namely  $s_i$ ,  $u_i$ , and b, are uniquely determined and independent of v as long as  $v < \beta_3$ .

**Proof.** Since route w is given, incentives  $\eta_w$  claimed by existing riders, and the payoff before accepting rider  $\hat{i}$  are both known. As rider  $\hat{i}$  must be accommodated, the total revenue after accepting  $\hat{i}$  is constant. After setting  $x_{ij} = \bar{x}_{ij}$ , the total driving distance  $\beta_1 \sum_{(i,j) \in A} c_{ij} \bar{x}_{ij}$  and total driving time  $\beta_2 \sum_{(i,j) \in A} t_{ij} \bar{x}_{ij}$  are further fixed. Only the vehicle idle cost and the incentive for the new rider remain in the optimization objective Eq. (1). Without loss of generality, we fix z at 1 (i.e., shifting the pickup time to be earlier). Then, BCP is reduced to a linear program:

(BCP-fixed) 
$$\max_{\{s_i, u_i, b\}} -\beta_3 \sum_{i \in P} s_i - vb$$
 (22)

s.t. 
$$u_i + s_i + \epsilon_i + t_{ii} - u_i = 0, \quad \forall (i, j) \in \bar{A}$$
 (23)

$$u_i - (u_i + s_i + \epsilon_i) \le R_{ii}, \quad \forall (i, j) \in B \tag{24}$$

$$e_i \le u_i + s_i \le l_i, \quad \forall i \in P \setminus \{\hat{i}\}$$
 (25)

$$0 \le s_i \le \bar{s}_i, \quad \forall i \in P \tag{26}$$

$$s_j = 0, \quad \forall j \in D \tag{27}$$

$$-b \le u_{\hat{i}} + s_{\hat{i}} - e_{\hat{i}}, \quad (\mu_{\hat{i}}) \tag{28}$$

$$b \le l_{\hat{i}} - u_{\hat{i}} - s_{\hat{i}}, \quad (\lambda_{\hat{i}}) \tag{29}$$

$$-b \le 0, \quad (\theta) \tag{30}$$

$$b \le \bar{b}. \quad (\xi) \tag{31}$$

In Eq. (23),  $\bar{A}$ , a subset of A, represents selected arcs, namely  $\bar{A} = \{(i,j) | x_{ij} = 1\}$ . When  $x_{ij} = 0$ , Eqs. (6) and (7) are superfluous, which can be removed from the reduced BCP.

We begin with a simple case where b = 0, meaning no schedule deviations. In this case, the optimization objective is to minimize the total idle cost, which is independent of b. Therefore, the values of  $s_i$  and  $u_i$  are uniquely determined by solving the linear program Eqs. (22) to (31) when b = 0.

Then, we analyze the case with schedule deviations, meaning b > 0. Note that b is not involved in Eqs. (23) to (27). Regardless of the shadow prices associated with those constraints, the reduced cost for variable b is written as follows:

$$\bar{c} = -v + \mu_{\hat{i}} - \lambda_{\hat{i}} + \theta - \xi. \tag{32}$$

As indicated after each of the last few constraints,  $\mu_{\hat{i}}$ ,  $\lambda_{\hat{i}}$ ,  $\theta$ , and  $\xi$  are nonnegative shadow prices for constraints (28), (29), (30), and (31), respectively.

As b is in the basis, due to b > 0, the reduced cost  $\bar{c}$  should be zero at optimality, which implies:

$$-v + \mu_{\hat{i}} - \lambda_{\hat{i}} + \theta - \xi = 0. \tag{33}$$

Since v is strictly positive, we must have:

$$\mu_{\hat{l}} + \theta > 0. \tag{34}$$

Since b > 0, the following complementary slackness condition about Eq. (30) implies  $\theta = 0$ :

$$b\theta = 0.$$
 (35)

Then, we derive a strictly positive  $\mu_i$  from Eq. (34). This further implies that Eq. (28) is binding, namely:

$$u_{\hat{i}} + s_{\hat{i}} + b = e_{\hat{i}}. \tag{36}$$

The above equation states that when the pickup time window is shifted for rider  $\hat{i}$ , the sum of  $s_{\hat{i}}$  and b should be optimized to meet the equality in Eq. (36). In other words, the vehicle's arrival time at node  $\hat{i}$  plus idle time plus schedule deviation equals the original left time window at the pickup location.

Further, note that the optimization objective Eq. (22) can be rewritten as:

$$\underset{\left\{s_{i},u_{i},b\right\}}{\operatorname{Max}} - \beta_{3} \sum_{i \in \backslash \left\{\hat{i}\right\}} s_{i} - \left(\beta_{3} s_{\hat{i}} + \upsilon b\right). \tag{37}$$

Since  $v < \beta_3$ , to maximize the objective Eq. (37), we must increase b while decreasing  $s_i$  at the same rate, subject to bounds on b and  $s_i$ , defined in Eqs. (31) and (26), respectively. Therefore, regardless of the value of v, if  $v < \beta_3$ , the optimal values of  $u_i$ ,  $s_i$ , and b are uniquely determined, independent of v.  $\square$ 

By summarizing the two cases, b = 0 and b > 0, we conclude that the values of continuous variables depend only on the values of discrete variables, independent of parameter v, on the condition that  $v < \beta_3$ , which is true in practice. Note that the hourly cost of idling a vehicle, namely  $\beta_3$ , is greater than the compensation rate v offered to a rider.

We then examine the behavior of the BCP's optimization objective.

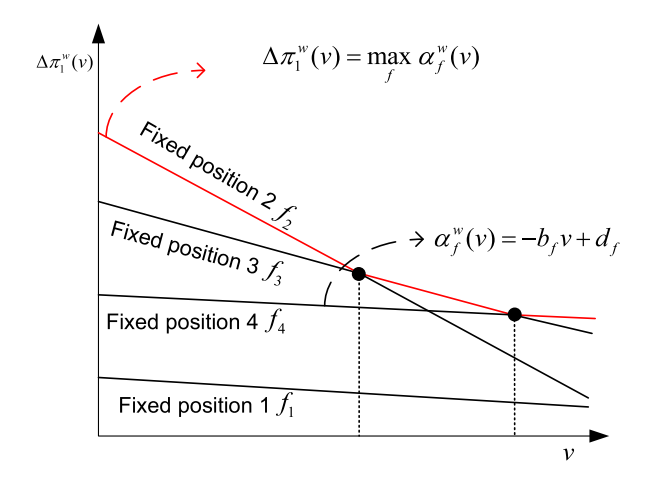


Fig. 3. Illustrative relation between  $\Delta \pi_1^w$  and v. (For interpretation of the references to color in this figure legend, the reader is referred to the web version of this article.)

**Proposition 2.** The optimization objective Eq. (1) is a piecewise linear decreasing function of v.

**Proof.** From Proposition 1, we know when discrete variables are fixed, denoted as a fixed position f,  $\Delta \pi_1^w$  reduces to a linear function of v, written as follows:

$$\alpha_f^w(v) = -b_f v + d_f, \tag{38}$$

where both the nonzero gradient  $-b_f$  and intercept  $d_f$  depend on the values of discrete variables f.

Then,  $\Delta \pi_1^w$  can be written as follows:

$$\Delta \pi_1^w(v) = \max_f \alpha_f^w(v). \tag{39}$$

Essentially, we would like to find the upper envelope (or pointwise maximum) of many linear segments. Fig. 3 illustrates how  $\Delta \pi_1^w(v)$  varies with v for a few different fixed positions (i.e., fixed values of discrete variables  $x_{ij}$  and z). Clearly, some fixed positions are completely dominated, while others are preferable partially, depending on v. The red segments (used interchangeably with pieces) constitute a continuous piecewise linear function, which is also the upper envelope.

As each linear function  $\alpha_f^w(v)$  decreases monotonically, the upper envelope  $\Delta \pi_1^w$  decreases monotonically, because any piece of the upper envelope is part of a linear function  $\alpha_f^w(v)$ . Furthermore, we show that the gradient  $-b_f$  increases (i.e.,  $b_f$  decreases) after each turning point. For a given intersection of two linear functions  $\alpha_f^w(v)$  and  $\alpha_{f'}^w(v)$ , we must have the following equality:

$$-b_f \hat{v} + d_f = -b_{f'} \hat{v} + d_{f'}. \tag{40}$$

Without loss of generality, we assume  $-b_f < -b_{f'}$ . When we slightly increase v to  $\hat{v} + \Delta_v$ , where  $\Delta_v$  is a small increment, the linear function with a larger gradient, namely  $\alpha_{f'}^w(v)$ , is selected to form a piece of the upper envelope, because

$$-b_{f}(\hat{v} + \Delta_{v}) + d_{f} < -b_{f'}(\hat{v} + \Delta_{v}) + d_{f'}. \tag{41}$$

At  $\hat{v} - \Delta_v$ ,  $\alpha_f^w(v)$  forms a piece of the upper envelope. Therefore, after the turning point  $\hat{v}$ , the gradient of a piece of  $\Delta \pi_1^u$  increases.  $\Box$ 

# 4.2. Solving N-BCP for fixed discrete variables

# 4.2.1. Concavity analysis

From Proposition 1, we know that  $\Delta \pi_1^w$  becomes a linear function of v with a slope of -b for fixed  $x_{ij}$  and z, as shown in Eq. (38). We next explore the objective of the negotiable BCP.

**Proposition 3.** The objective  $\mathbb{E}(\Delta x^w)$  defined in Eq. (21) is strictly concave in v when fixing  $x_{ij}$  and z.

**Proof.** The first-order partial derivative of the objective  $\mathbb{E}(\Delta \pi^w)$  with respect to v is as follows:

$$\frac{\partial \mathbb{E} \left( \Delta \pi^{w} \right)}{\partial v} = \boldsymbol{\Phi}' \left( \frac{v - \mu}{\sigma} \right) \frac{1}{\sigma} \left( \Delta \pi_{1}^{w} - \Delta \pi_{0}^{\text{max}} \right) - \boldsymbol{\Phi} \left( \frac{v - \mu}{\sigma} \right) b, \tag{42}$$

where  $\Phi'\left(\frac{v-\mu}{\sigma}\right)$  is the probability density function (PDF) for the normal distribution.

The second-order partial derivative is:

$$\frac{\partial^{2} \mathbb{E} \left( \Delta \pi^{w} \right)}{\partial v^{2}} = \boldsymbol{\Phi}^{"} \left( \frac{v - \mu}{\sigma} \right) \frac{1}{\sigma^{2}} \left( \Delta \pi_{1}^{w} - \Delta \pi_{0}^{\max} \right) - \boldsymbol{\Phi}^{'} \left( \frac{v - \mu}{\sigma} \right) \frac{b}{\sigma} - \boldsymbol{\Phi}^{'} \left( \frac{v - \mu}{\sigma} \right) \frac{b}{\sigma}, \tag{43}$$

which is rearranged as:

$$\frac{\partial^{2} \mathbb{E} \left( \Delta \pi^{w} \right)}{\partial v^{2}} = \Phi'' \left( \frac{v - \mu}{\sigma} \right) \frac{1}{\sigma^{2}} \left( \Delta \pi_{1}^{w} - \Delta \pi_{0}^{\max} \right) - 2\Phi' \left( \frac{v - \mu}{\sigma} \right) \frac{b}{\sigma}. \tag{44}$$

As the PDF  $\Phi'\left(\frac{v-\mu}{\sigma}\right)$  is always positive,  $\sigma>0$ , and  $b\geq0$ , the second expression  $-2\Phi'\left(\frac{v-\mu}{\sigma}\right)\frac{b}{\sigma}\leq0$ . Since  $\Phi'\left(\frac{v-\mu}{\sigma}\right)$  is monotonically decreasing when  $v>\mu$ , the second-order partial derivatives  $\Phi''\left(\frac{v-\mu}{\sigma}\right)$  is always negative. By further noting  $\Delta\pi_1^w>\Delta\pi_0^{\max}$ , the first expression  $\Phi''\left(\frac{v-\mu}{\sigma}\right)\frac{1}{\sigma^2}\left(\Delta\pi_1^w-\Delta\pi_0^{\max}\right)<0$ . Overall, the second-order partial derivatives  $\frac{\partial^2\mathbb{E}(\Delta\pi^w)}{\partial v^2}$  is negative and the objective  $\mathbb{E}\left(\Delta\pi^w\right)$  is strictly concave in v for any fixed values of  $x_{ij}$  and z.  $\square$ 

We next explain how  $\mathbb{E}(\Delta\pi^w)$  varies when v increases from  $v_{\min}$  to  $\bar{v}$  and discrete variables are fixed at f. Clearly, the acceptance probability  $\Phi\left(\frac{v-\mu}{\sigma}\right)$  increases monotonically with v and  $\left(\Delta\pi_1^w-\Delta\pi_0^{\max}\right)$  decreases linearly with v at the rate of b, as shown in Eq. (38). When  $v=v_{\min}$ ,  $\mathbb{E}(\Delta\pi^w)$  is the average of  $\alpha_f^w\left(v_{\min}\right)$  and  $\Delta\pi_0^{\max}$ , because  $\Phi\left(\frac{v-\mu}{\sigma}\right)=0.5$  and  $v_{\min}=\mu$ . When v increases, the acceptance probability is greater than 0.5 and the linear function Eq. (38) becomes an asymptote of  $\mathbb{E}(\Delta\pi^w)$ , which means the difference between  $\alpha_f^w\left(v\right)$  and  $\mathbb{E}(\Delta\pi^w)$  approaches zero. When optimizing v, a tradeoff between the acceptance probability and cost of incentives should be balanced.

# 4.2.2. Optimizing v for fixed discrete variables

Fixing discrete variables reduces  $\mathbb{E}(\Delta \pi^{w})$  to a single-variate nonlinear function of v. An exhaustive search on the interval  $\left[v_{\min}, \bar{v}\right]$  yields the optimal v. Nonetheless, we can avoid this complete enumeration approach by utilizing the concavity of  $\mathbb{E}(\Delta \pi^{w})$ , stated in Proposition 3.

After fixing discrete variables at f and dropping constant  $\Delta \pi_0^{\text{max}}$ , the N-BCP is rewritten as:

$$\operatorname{Max}_{v} \Phi\left(\frac{v-\mu}{\sigma}\right) \left(\alpha_{f}^{w}\left(v\right) - \Delta \pi_{0}^{\max}\right) \tag{45}$$

$$s.t. \quad v_1^f \le v \le v_2^f \tag{46}$$

The interval  $\left[v_1^f, v_2^f\right]$  is specific to the fixed position f, and Section 4.3.1 presents an approach for determining it for a given f. Due to the concavity of the objective Eq. (45), the nonlinear program Eqs. (45) and (46) is equivalent to the following linear program:

$$\max_{\{p,q\}} \alpha \tag{47}$$

s.t. 
$$\alpha \le g_k (v - v_k) + \alpha_k, \forall k \in K$$
 (48)

$$v_1^f \le v \le v_2^f \tag{49}$$

In Fig. 4, each linear function approximates the concave function at a specific value of v, corresponding to one of constraints (48). For instance, when  $v = v_k$ , the nonlinear program Eqs. (45) to (46) reduces to a linear one, resulting in an optimal objective of  $\alpha_k$ . Gradient  $g_k$  is given by Eq. (42) for given  $v_k$ . Essentially,  $\alpha = g_k \left( v - v_k \right) + \alpha_k$  is a tangent line to the nonlinear curve at  $v_k$ . Due to the concavity of the curve, we have constraints (48).

We next describe how those constraints can be generated sequentially. To initialize, two tangent lines are produced for  $v_1^f$  and  $v_2^f$ . A new tangent line or value of v can be found as follows: solve the linear program Eqs. (47) to (49) considering all tangent lines generated so far and the optimum  $v^*$  is used to find the next tangent line. The above procedure terminates when the difference between two consecutive v values is smaller than a tolerance, i.e.,  $|v_k - v_{k-1}| \le \epsilon_v$ , where  $\epsilon_v$  is a predefined tolerance. Then, the optimum v is found. The above approach for optimizing v is more efficient than the exhaustive search as it avoids a direct enumeration of all possible v values on an interval.

# 4.3. Optimizing fixed positions

#### 4.3.1. Generation of piecewise linear function

In Section 4.2, the discrete variables, specifically  $x_{ij}$  and z, are fixed at the position f. In this section, we detail the process for optimizing these discrete variables, which entails the selection of the appropriate fixed position f.

A pre-screening technique based on time window checking can be introduced to exclude infeasible f. Without loss of generality, we assume z=1, which means the pickup time window for the new rider  $\hat{i}$  is  $\left[e_i-b,l_i-b\right]$ , where b is between 0 and  $\bar{b}$ . For each existing arc (i,j), a pickup or drop-off location of the new rider  $\hat{i}$  cannot be inserted between i and j, when any of the following conditions are met:

$$e_i + \epsilon_i + t_{j\hat{i}} > l_{\hat{i}} \tag{50}$$

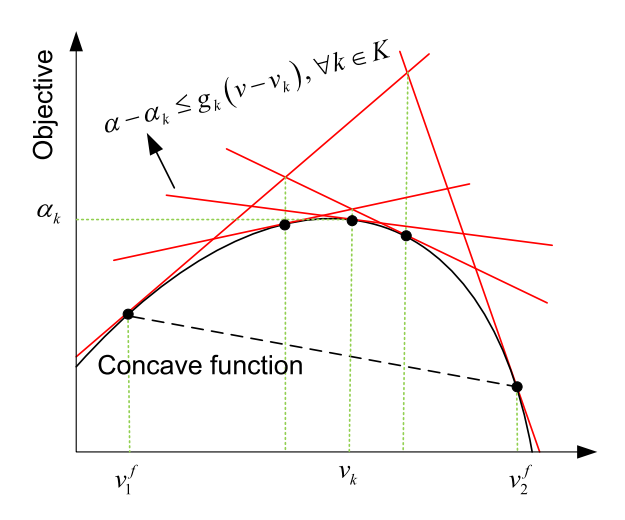


Fig. 4. Linear approximation of concave function.

$$l_i + \epsilon_i + t_{\hat{i}\hat{i}} < e_{\hat{i}} - b \tag{51}$$

$$e_{\hat{l}} - b + \epsilon_{\hat{l}} + t_{\hat{l}\hat{l}} > l_{\hat{l}} \tag{52}$$

$$l_{\hat{i}} + \epsilon_{\hat{i}} + t_{\hat{i}i} < e_{\hat{i}}. \tag{53}$$

Essentially, if there is no overlap between the negotiable time window and other time windows after adjustments for service duration and link travel time, the fixed position is infeasible.

Algorithm 1 describes the process for deriving the upper envelope illustrated in Fig. 3.

# Algorithm 1. Derivation of upper envelope for fixed positions

Input: Set of all feasible fixed positions F

Output: Piecewise linear function

Set  $v_1 = v_{\min}$ 

while  $F \neq \emptyset$  do

Find position f with the highest intercept, i.e.,  $d_f$  defined in Eq. (38)

Remove from F those positions with a smaller gradient than  $-b_f$  as defined in Eq. (38)

Identify the next position with the second-highest intercept

Compute intersection with  $\alpha_f^w(v)$  to get  $v_2^f$ 

Identify f as the dominating fixed position over  $\left|v_1, v_2^f\right|$ 

 $F \leftarrow F \setminus \{f\}$ 

Update interval for v to  $\left[v_2^f, \bar{v}\right]$ , namely setting  $v_1 = v_2^f$ 

end while

Each piece of the output corresponds to a dominating fixed position f

return Piecewise linear function

Algorithm 1 produces a piecewise linear function. Each segment (equivalently piece) of this function corresponds to a dominating fixed position f, namely specific values of discrete variables  $x_{ij}$  and z. For the segment specific for f, v spans the interval  $\left[v_1^f, v_2^f\right]$ . Since the number of segments is finite and the optimal solution for each can be determined using the approach detailed in Section 4.2, the global optimum for the N-BCP can be found by exhaustively evaluating each segment.

#### 4.3.2. Segment equivalence and dominance

While evaluating each segment of an obtained piecewise linear function yields the optimum fixed position, some segments can be eliminated by an indifference curve, to be defined and described as follows.

For an initial segment of a piecewise linear function, namely a fixed position f, the N-BCP can be solved optimally using the solution approach given in Section 4.2. The optimal v and the optimum objective are denoted as  $v_f^*$  and  $\zeta_f^*$ , respectively. From this

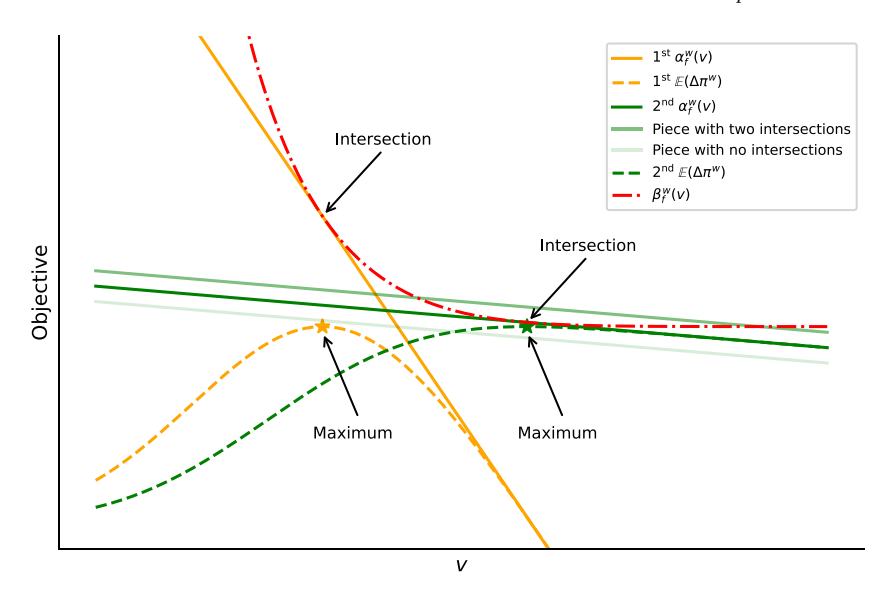


Fig. 5. An indifference curve with two equivalent solutions.

optimum solution, we derive the following function of v:

$$\beta_f^w(v) = \frac{\zeta_f^* - \Delta \pi_0^{\text{max}}}{\Phi\left(\frac{v - \mu}{\sigma}\right)} + \Delta \pi_0^{\text{max}}.$$
 (54)

In Eq. (54), only the acceptance probability  $\Phi\left(\frac{v-\mu}{\sigma}\right)$  varies with v, which is a concave function in v. It is thus easy to show that the indifference curve  $\theta_f^w(v)$  is convex as  $\Phi\left(\frac{v-\mu}{\sigma}\right)$  is a denominator in Eq. (54).

**Proposition 4.** If one segment of the given piecewise linear function, e.g.,  $\alpha_{f'}^w(v)$  over interval  $\left[v_1^{f'}, v_2^{f'}\right]$ , has one and only one intersection with the function  $\beta_f^w(v)$ , an equivalent solution with the same objective value as  $\zeta_f^*$  can be found.

**Proof.** As  $\alpha_{f'}^{w}(v)$  has a single intersection with  $\alpha_{\min}^{w}(v)$ , we have the following:

$$\alpha_{f'}^w(v_{f'}) = \alpha_{\min}^w(v_{f'}), \tag{55}$$

where  $v_{f'}$  is the value of v at the intersection. For fixed position f' and the v value of  $v_{f'}$ , the objective of the N-BCP is computed as:

$$\mathbb{E}\left(\Delta \pi^{w}\right) = \Phi\left(\frac{v - \mu}{\sigma}\right) \left(\alpha_{f'}^{w}\left(v_{f'}\right) - \Delta \pi_{0}^{\max}\right) + \Delta \pi_{0}^{\max},\tag{56}$$

which is exactly  $\zeta_f^*$  after noting Eqs. (54) and (55).  $\square$ 

Fig. 5 shows such a case where the indifference curve intersects with another segment at a single point. Two equivalent solutions with the same payoff are thus shown. The second segment cannot be eliminated and must be evaluated to find a possibly superior solution. Fig. 5 also shows that for fixed discrete variables (i.e., a single segment), the optimization problem reduces to a convex optimization problem consisting of continuous variables only, while the optimization problem is nonconvex when discrete variables are optimized simultaneously with continuous variables. Fig. 5 shows that the objective  $\mathbb{E}(\Delta \pi^w)$  is a nonconvex function of v when two segments are considered simultaneously rather than fixing one of them. Motivated by this observation, a decomposition-based solution approach will be designed and presented in Section 4.4.

If  $\alpha_{f'}^w(v)$  has two intersections with the indifference curve  $\zeta_f^*$ , i.e.,  $\alpha_{f'}^w(v) > \beta_f^w(v)$  over a certain interval for v illustrated in Fig. 5, it is likely that a higher payoff than  $\zeta_f^*$  can be achieved over an interval for v. When no intersections exist between  $\zeta_f^*$  and  $\alpha_{f'}^w(v)$ , the fixed position f' is dominated, and there is no need to evaluate it. Thus, the indifference curve can be used to eliminate some fixed positions (or pieces of the piecewise linear function).

It should be noted that, on a two-dimensional plane, the possible number of intersections between a strictly convex function and a linear function can only be 0, 1, or 2. Additionally, solving a system of two equations can determine the number of intersections.

#### 4.4. Fix-and-optimize solution approach and optimality

In the N-BCP, we jointly optimize routing, scheduling, and compensating decisions, considering the uncertain behavior response of a rider possessing private information. The resulting mathematical program is a nonconvex MINLP that cannot be directly solved by any commercial solvers, making it impossible to guarantee the quality of the solution. We next present a fix-and-optimization solution approach after decomposing all decisions into continuous and discrete and explain why this approach ensures that the returned solution is optimal.

With the procedure stated in Section 4.3.1, a piecewise linear function is achieved, whose first segment with the largest intercept determines the initial fixed position. The approach in Section 4.2 is then used to optimally solve the N-BCP for fixed discrete variables. The obtained optimum solution yields an indifference curve, which can be used to determine whether other segments of the piecewise linear function should be explored. If so, the corresponding N-BCP is solved. The solution process ends when all segments are evaluated or eliminated.

In the above fix-and-optimize strategy, it is important to highlight two key observations. First, for each segment related to a fixed position of discrete variables, the reduced N-BCP is solved to optimality, as demonstrated in Section 4.2. Second, every conceivable fixed position has been either explicitly assessed or ruled out, as elaborated in Section 4.3. Consequently, our proposed method is assured to yield an optimal solution. To encapsulate this conclusion, we formalize the following result:

**Proposition 5.** The fix-and-optimize solution method yields an optimal solution for the N-BCP.

#### 5. Case studies

We present two sets of computational experiments to demonstrate the proposed optimization method and evaluate the impact of schedule negotiation on ADA paratransit operations. The first set of experiments is based on synthetic data, while the second is for a paratransit operator based in a Washington, D.C. suburb. All computations are conducted on a personal computer (i7-10700K Processor @ 3.80 GHz and 32 GB RAM).

#### 5.1. Synthetic instances

#### 5.1.1. Travel demand data

Each rider's pickup and drop-off locations are randomly sampled from a 20 by 20 square region. The requested pickup time  $\zeta_i^p$  of rider i is uniformly distributed over [60, 480], which is part of a planning horizon of [0, 600]. As the minimum advance booking time is 30, a booking can be submitted anytime between 30 and  $\zeta_i^p - 30$ . The pickup time window  $[e_i, l_i]$  is constructed as  $e_i = \zeta_i^p - 10$  and  $l_i = \zeta_i^p + 10$ . The service duration  $e_i$  is 3. A maximum ride time of 90 is imposed. The travel time  $t_{ij}$  between any two nodes i and j is estimated as the Euclidean distance  $c_{ij}$  divided by the average travel speed of 1. When computing the operating cost, the coefficients for the driving distance, driving time, and idle time are specified as 1.3, 0.3, and 0.4, respectively. The service revenue for a rider is estimated at 1.1 times the cost of providing an exclusive (non-sharing) ride to this rider. The true VoT of a rider is randomly sampled from a normal distribution with  $\mu = 15$  and  $\sigma = 1$ . In total, 100 riders or bookings are generated with the above procedure.

#### 5.1.2. Booking confirmation instances

After sorting all bookings by booking time, the first 20 bookings are selected as subscription trips, which are assumed to be confirmed already and thus known at the current time. A widely used routing heuristic developed by Jaw et al. (1986) is used to accommodate those bookings, producing five routes. The remaining 80 trips are considered non-subscription or on-demand, which are subject to schedule negotiations.

We construct one booking confirmation instance for each on-demand rider as follows. Right after receiving an on-demand booking, an instance consisting of all existing vehicle routes covering all confirmed riders and the underlying new rider is solved. The proposed schedule deviation and accompanying incentive are presented to the rider for decision. Depending on the rider's response, the booking is confirmed with or without schedule deviations, and a new set of existing vehicle routes becomes available, which becomes the initial set of routes for the next instance. An instance should be solved quickly, e.g., within one or two minutes of booking time, as the rider waits for the confirmation. Since there are 80 non-subscription bookings, 80 instances are built and solved.

During negotiations, the following parameters are used:  $\bar{b} = 30$ ,  $v_{\min} = \mu$ , and  $\bar{v} = \mu + 3\sigma$ .

# 5.1.3. Solution to one problem instance

For example, we examine the 26th instance, which involves 10 existing routes covering 45 confirmed bookings and a new rider. Table 2 shows that only two (namely routes 0 and 7) among the 10 routes can feasibly accommodate the new rider, when schedule deviations are not permitted, indicated by column  $4\pi_0^w$ . Among the two, route 0 is the preferred one, which yields a payoff of \$18.2. When schedule deviations are possible and the new rider is fully compliant, corresponding to column  $4\pi_1^w$ , two additional routes (i.e., routes 2 and 9) can further accommodate the new rider. Schedule negotiations are unnecessary for routes 0 and 7 as the resulting payoff under full compliance does not exceed \$18.2, the highest payoff achieved without schedule deviations. Therefore, for each of all other feasible routes (i.e., routes 2 and 9), the N-BCP problem is solved and the expected payoff is recorded in

Table 2
Illustrative booking confirmation instance.

w	$\Delta\pi_0^w$	$\Delta\pi_1^w$	$\mathbb{E}\left(\Delta\pi^{w}\right)$	$\Phi\left(\frac{v-\mu}{\sigma}\right)$	vb	Negotiate?
0	18.2	18.2				
2		28.3	27.6	0.989	4.93	Yes
7	2.8	7.3				
9		19.1	18.7	0.617	7.65	
Other routes						

The blank cells indicate the unattainable values caused by infeasibility.

Table 3
Result summary of solving all instances for one random seed.

Payoff before N. (\$)	Payoff after N. (\$)	#N.	#S.N.	Total incentive (\$)
4292.1	4434.8	42	41	160.9

<sup>&</sup>quot;N." means negotiation. "S.N." means successful negotiations.

column  $\mathbb{E}(4\pi^w)$ . Clearly, route 2 provides the highest expected value at \$28.3. The acceptance probability is 98.9%, which is very high because \$28.3 (payoff when the rider accepts the proposal) is significantly larger than \$18.2 (payoff otherwise). Therefore, route 2 should be selected for negotiation. Despite the high expected acceptance probability, the rider may decline it due to the private VoT information.

Allowing schedule negotiations leads to an expected payoff of \$27.6, while the payoff is \$18.2 otherwise. The cost reduction is larger than \$9.4 (i.e., \$27.6 - \$18.2) after adjusting for the needed compensation vb multiplied by  $\Phi\left(\frac{v-\mu}{\sigma}\right)$ , which is \$4.88. The expected ROI (Return on Investment) is (\$27.6 - \$18.2)/\$4.88 = 1.93.

#### 5.1.4. Effectiveness of schedule negotiation

We note that in the 26th instance, schedule negotiations are beneficial. In some other instances, negotiating for a different pickup time window may not be justified. In such a case, no incentives are needed, and the new rider is accommodated without a schedule deviation.

Each point in Fig. 6 represents an instance for which schedule negotiations are conducted. The *x*-axis represents incentives offered to the new rider (i.e., investment), and the *y*-axis represents incremental payoffs should the incentives be accepted (i.e., return). The 26th instance analyzed earlier is highlighted. It can be seen that significantly higher or lower returns can be expected in other instances. The average ROI is computed as 4.1, which means one dollar of incentive is expected to yield 4.1 dollars of return.

We also use five other random seeds and explore the ROI distribution. Fig. 7 presents the distributions of ROIs of all negotiations for five random seeds. Generally, the average ROI for each individual negotiation is around 3.5, which means the benefits of schedule negotiations are substantial and quite robust.

#### 5.1.5. Usefulness of future booking information

For a given random seed, out of 42 negotiation instances, 41 riders eventually accepted the proposal, as shown in Table 3. The total incentives paid to those riders over the 41 instances were \$160.9, and the net payoff improvements were \$142.7, which implies that the ROI is 0.9. First, the ROI is positive, which means after solving all those instances over time, schedule negotiations can yield net payoff improvements. More importantly, this ROI of 0.9 is significantly lower than 3.5, the average ROI for each individual instance. This dramatic ROI decrease can be attributed to the neglect of interrelations among successive negotiation instances, elaborated as follows.

The schedule negotiation problem instance is built and solved for each incoming rider separately, with no knowledge of future riders and no consideration of the current decision's impact over future ones. In other words, as the operator cannot predict the next booking, it optimizes its decision locally instead of globally over time. This shortsighted decision, which yields high ROIs for individual instances, may turn out to be less effective when the effectiveness of such decisions is examined over time. For instance, we shifted rider 1's schedule to be earlier; then it was found that rider 1's schedule could be moved in an opposite direction to accommodate a new rider, who has the same origin as rider 1 but a different time preference. Extending the current static negotiation to consider complexities arising from a dynamic and stochastic environment is clearly a future research need.

# 5.1.6. Efficiency of proposed solution approach

The efficiency of the proposed fix-and-optimize solution approach is evaluated by solving the 42 instances for a given random seed. For comparison, we consider a baseline algorithm that enumerates all possible values of discrete variables and evaluates v at a step size of 0.001 for each value of discrete variables. To ensure the same precision, the convergence tolerance  $\epsilon_v$  in Section 4.2.2 is also 0.001. Since each instance consists of multiple routes, the computation time reflects the total time for solving multiple N-BCPs. The baseline algorithm takes an average of 241.1 s for confirming each rider. Conversely, our proposed algorithm reduces these tasks to an average of 21.9 s. Fig. 8 shows the distribution of ratios of total computation time for solving each instance, in which insertions into multiple routes are involved. The proposed fix-and-optimize approach reduces the total computation time by 91.5% compared to the baseline algorithm, attesting to its efficiency. It is worth noting that the proposed solution approach yields the globally optimal solution, which is validated by the optimum achieved by the baseline algorithm.

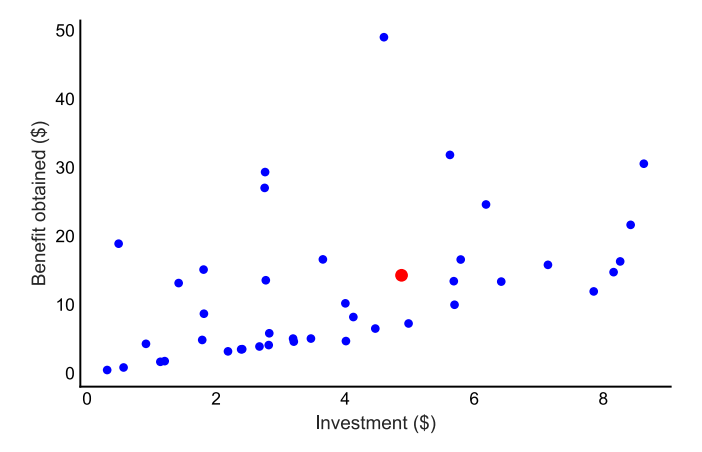


Fig. 6. Comparison of benefits and incentives in all intended negotiations.

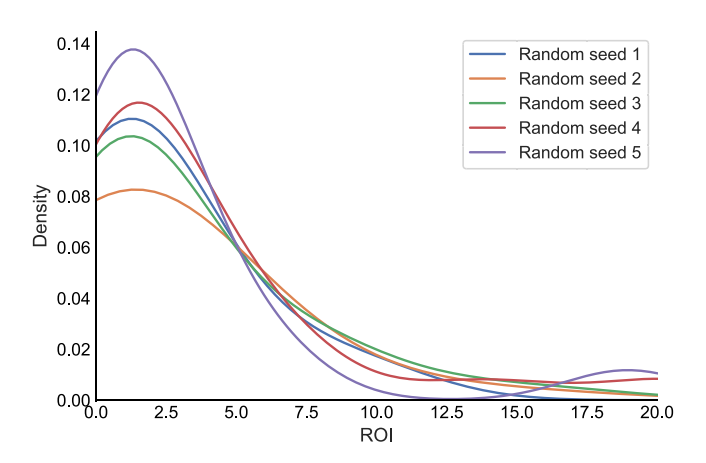


Fig. 7. Distributions of ROIs in successful negotiations.

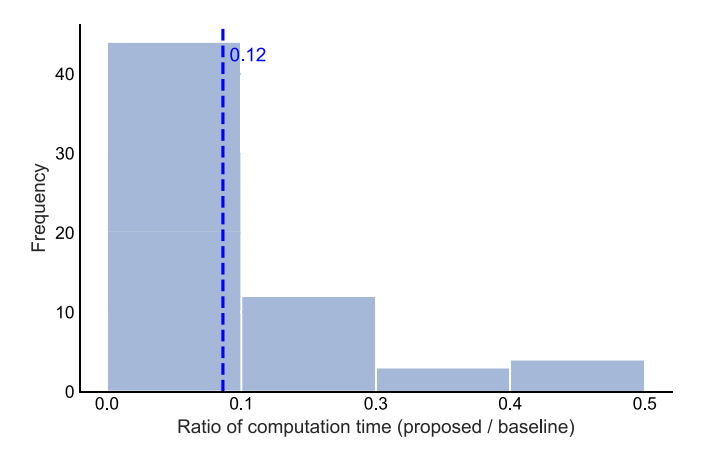


Fig. 8. Comparing computation time.

# 5.2. Real-world instances

#### 5.2.1. Data and experimental setting

The empirical study employs a trip dataset from Challenger Transportation, which is a subcontractor of the Washington Metropolitan Area Transit Authority (WMATA) for providing ADA paratransit services in the Maryland-District of Columbia region. This dataset has essential attributes of each paratransit trip, such as the pickup and drop-off locations and requested pickup time.

 Table 4

 Baseline values of parameters in real-world instances.

Parameter	Value	Parameter	Value
μ	\$15/h	$\epsilon_i$	3 min
$\sigma$	\$2/h	$R_{ij}, \forall (i,j) \in B$	$\max\{60,3t_{ij}\}$ min
$v_{\rm min}$	\$15/h	$\boldsymbol{\beta}_1$	\$1.3/mile
$\bar{v}$	\$21/h	$\beta_2$	\$0.3/min
$ar{b}$	60 min	$oldsymbol{eta}_3$	\$0.4/min

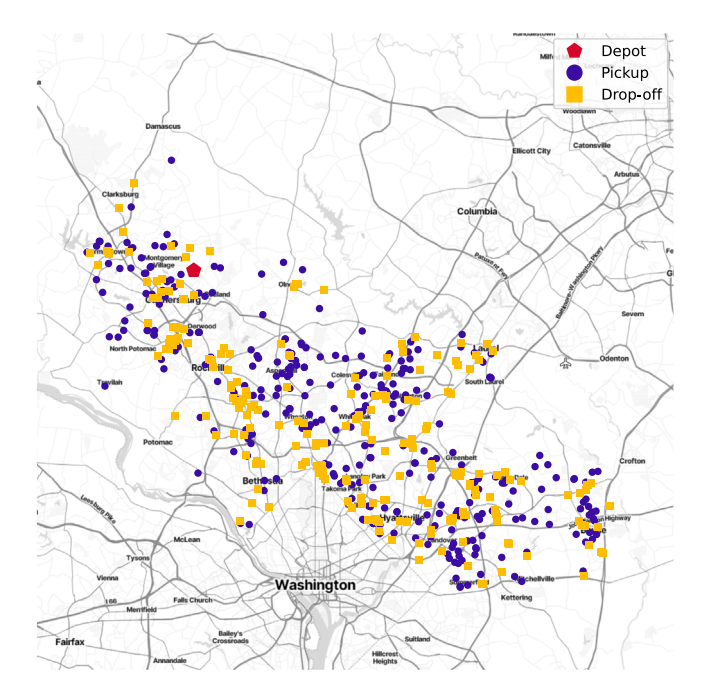


Fig. 9. Pickup and drop-off locations of the 337 trips.

We select a subset of trips with a pickup time between 6 am and 10 am on January 15, 2022. Fig. 9 visualizes the pickup and drop-off locations for those selected 337 trips, and vehicle depot.

The booking time is unavailable to the subcontractor as WMATA has a centralized call center. To enrich the dataset, booking time is sampled randomly from the interval  $\left[240,\zeta_{\hat{i}}^p-90\right]$  (unit: min), where  $\zeta_{\hat{i}}^p$  is the requested pickup time in trip i. By regulations, the width of the pickup time window is 30 min, and the maximum deviation  $\bar{b}$  is 60 min. The travel time and cost matrices are also given. Table 4 lists baseline values of other parameters, which are being used in the Mobile Resources Management System (MRMS) developed by IT Curves and applied in the daily operations of the clients of IT Curves. As those parameters and settings are largely based on the paratransit practice in the D.C. region, paratransit operators in other regions could customize those parameters to reflect their local conditions. Additionally, the revenue is estimated as 1.1 times the non-sharing travel cost for each rider, which might vary across regions. Nonetheless, the total revenue is constant because none of the travel requests can be rejected by the operator. A change in the revenue rate does not affect the subsequent optimization.

Like the synthetic instances in Section 5.1, all 337 riders are sorted by their booking time  $\tau_i$ . Among all riders, 20% of them (i.e., 67 riders) with the earliest booking times are considered as subscription trips and routed by a heuristic by Jaw et al. (1986), producing the initial set of routes. We first assume that the operator sequentially accommodates each of the 270 sorted riders without any negotiations. This way, each incoming rider yields an individual schedule negotiation instance, which needs to be solved by the proposed negotiation method. Those 270 instances are consistent regardless of the values of key parameters to be analyzed next, such as  $\mu$  and  $\bar{b}$ . In addition, a later instance does not depend on the choice of a rider who called in earlier. Those 270 instances are also fixed over different random seeds.

# 5.2.2. Benchmarking with a simplified negotiation policy

The proposed N-BCP is a nonconvex MINLP requiring a sophisticated solution algorithm. We intend to contrast it with a greatly simplified schedule negotiation policy, which provides a standard compensation rate the same as the mean VoT. In other words, we always set  $v = \mu$  under the simplified policy, effectively reducing the MINLP to MIP.

Under both policies, schedule negotiations are conducted in 119 out of 270 instances. Fig. 10 shows the expected incentive claimed by riders and expected return under both policies for each of the 119 instances. The expected incentive is *vb* multiplied by

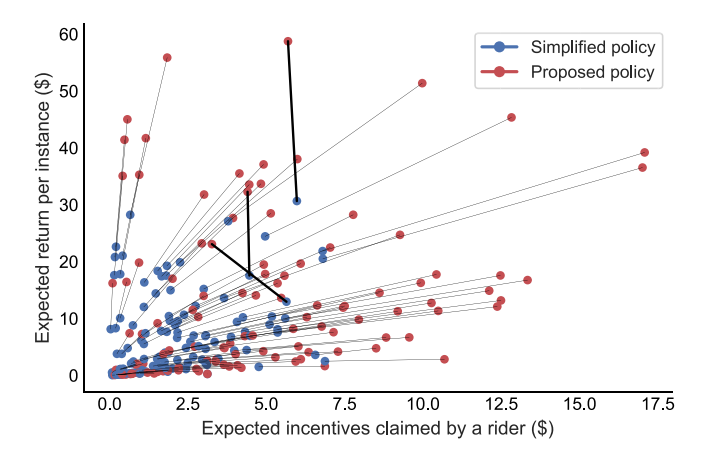


Fig. 10. Comparative advantage of the proposed policy.

Table 5
Performance comparison of two negotiation policies in solving each instance.

Policy	v (\$/h)	b (min)	vb (\$)	Acceptance Prob. $\phi$	Expected return (\$)
Simplified	15.0	17.1	4.3	0.50	7.1
Proposed	18.7	16.0	4.9	0.93	12.9

the acceptance probability  $\phi$ . The expected return is the expected payoff with negotiations minus the payoff without negotiations, namely  $\mathbb{E}(\Delta\pi^w) - \Delta\pi_0^w$ . In most instances, the expected incentive is higher under the proposed policy. In rare instances (3 out of 119), the expected incentive under the simplified policy is higher, because the proposed schedule deviations are excessive under the simplified policy. Those rare instances are highlighted by thick arcs in Fig. 10. We also observe that in all 119 instances, the proposed policy yields a higher expected return.

Table 5 further compares both policies by the mean values of a few metrics over 119 instances. Under the proposed policy, a higher compensation rate and a smaller deviation are offered. The total incentives offered in each instance are also higher under the proposed policy, although the incentive difference between the two policies is not significant. Nonetheless, the deviation acceptance probability under the simplified policy is only 50%, which leads to a much lower expected return under the simplified policy.

We simulate a rider's acceptance behavior ten times with different random seeds and measure the actual return. The cumulative returns over all instances under the proposed and simplified policies are \$1536.7 and \$838.6, respectively. The 83.2% higher return clearly demonstrates the superiority of the proposed policy.

# 5.2.3. Sensitivity analysis of $\mu$

We first examine the impact of  $\mu$  on the optimization results in a single instance, namely instance #7 involving rider 437 as the new rider. When  $\mu$  is relatively small, e.g., \$4.0/h, Fig. 11 shows rider 437 can be feasibly picked up before dropping off rider 459 after a schedule deviation is implemented. For each rider, a horizontal line represents trip duration, whose two endpoints correspond to optimized pickup and drop-off times, respectively. As shown in Fig. 11, rider 437's pickup is shifted by 53.5 min. When  $\mu$  increases, this schedule deviation remains optimal until a threshold of \$5.6/h is reached. As shown in Fig. 12 and before the \$5.6/h threshold,  $\nu$  and  $\nu$ b increase linearly with  $\mu$ ; the acceptance probability, expected return, and payoff all decrease accordingly.

When  $\mu$  increases beyond the threshold, accommodating rider 437 in a different route and with a different deviation becomes desirable. Fig. 13 shows that rider 437 can be feasibly picked up after dropping off rider 419 and before dropping off rider 422, subject to a deviation of 17.4 min. As a completely different route is selected for accommodating rider 437, all key decisions, such as v, b, and  $\phi$ , change dramatically, implying disjoint curves. At the \$5.6/h threshold, one is indifferent between two routes, which explains continuous curves for expected return and payoff.

The above analyses of instance #7 indicate that as the mean of VoT increases, different routes and schedule deviations could be suggested for the same rider. Understandably, in some other instances, there could be only one feasible route, and the proposed schedule deviation does not vary with  $\mu$ .

As the same analysis can be performed for each instance, Table 6 shows how the averages of a few key metrics over all instances vary with  $\mu$ . For both policies, as  $\mu$  increases, the magnitude of schedule deviation b decreases. Due to the sharp increase in the offered compensation rate v, the incentives offered in one instance vb increase as well. The acceptance probability slightly increases in the proposed policy while the expected return per instance is relatively stable for both policies. When two policies are contrasted, the expected return of the simplified policy is significantly (around 45%) lower than the proposed one, regardless of the value of  $\mu$ , in line with the comparison for a single instance presented earlier. The robustness of the proposed policy's advantage over the implied one is thus clear. For the proposed policy, we further note that the percentage of instances identified for negotiation becomes smaller as  $\mu$  grows, as shown in Fig. 14. This explains how the cumulative returns over all instances drop as  $\mu$  increases. This is

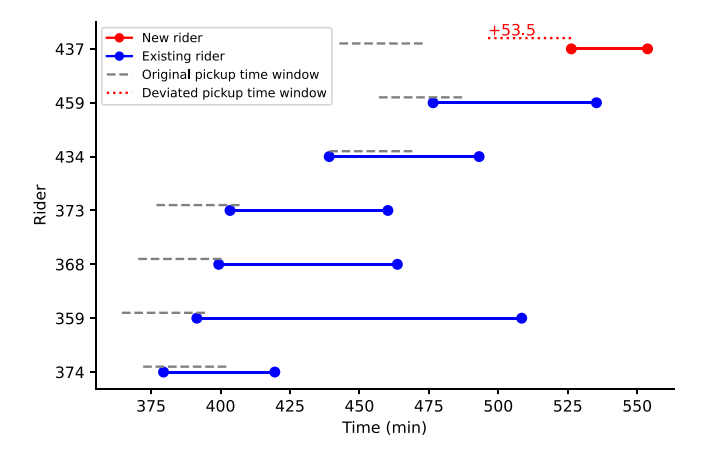


**Fig. 11.** Generated route when  $\mu = $4.0/h$ .

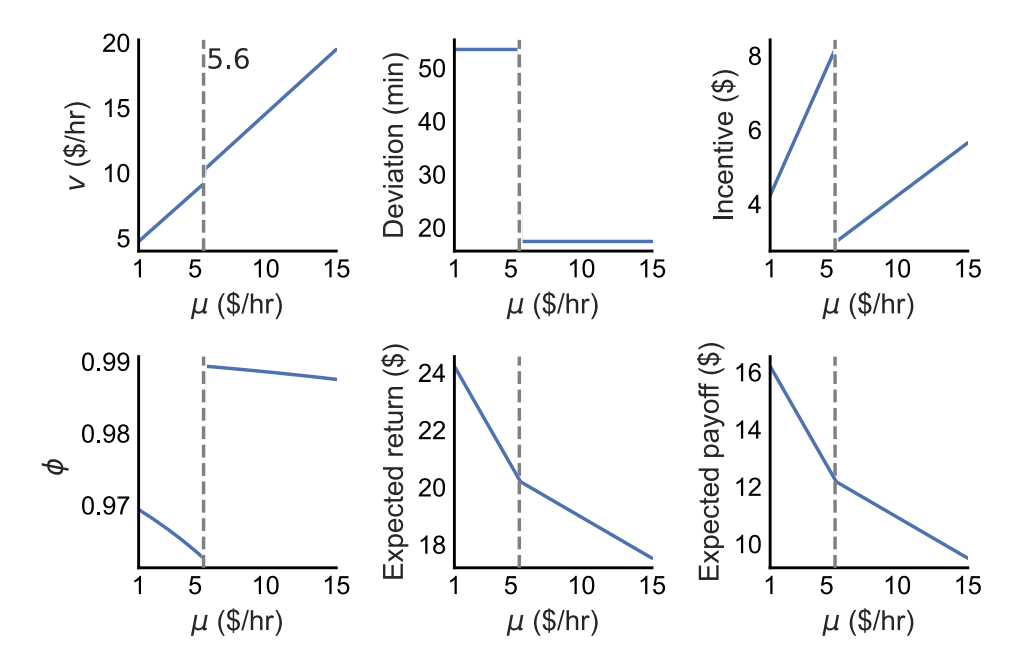
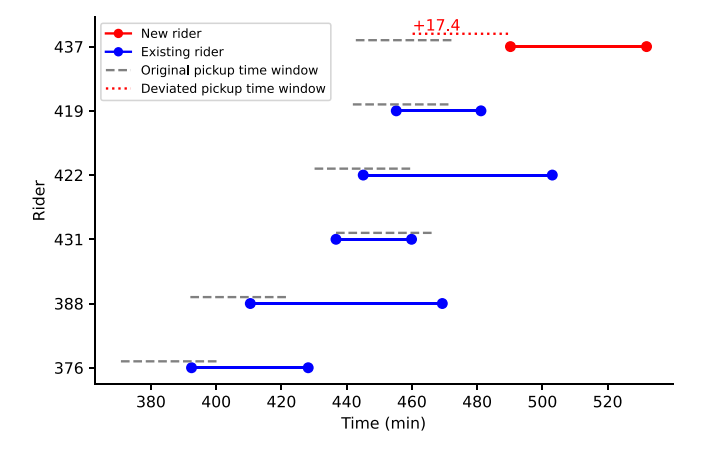


Fig. 12. Impacts of  $\mu$  on negotiation results in one instance.



**Fig. 13.** Generated route when  $\mu = 12.0/h$ .

**Table 6** Further comparison of two policies under various values of  $\mu$ .

μ (\$/h)	\$/h) Simplified policy					Proposed	policy			
	v (\$/h)	b (min)	vb (\$)	Acceptance Prob. $\phi$	Expected return (\$)	v (\$/h)	b (min)	vb (\$)	Acceptance Prob. $\phi$	Expected return (\$)
1	1	27.6	0.5	0.50	7.0	4.2	25.9	1.6	0.90	12.7
7	7	21.8	2.5	0.50	7.0	10.5	21.1	3.5	0.91	12.9
15	15	17.1	4.3	0.50	7.1	18.7	16.0	4.9	0.93	12.9

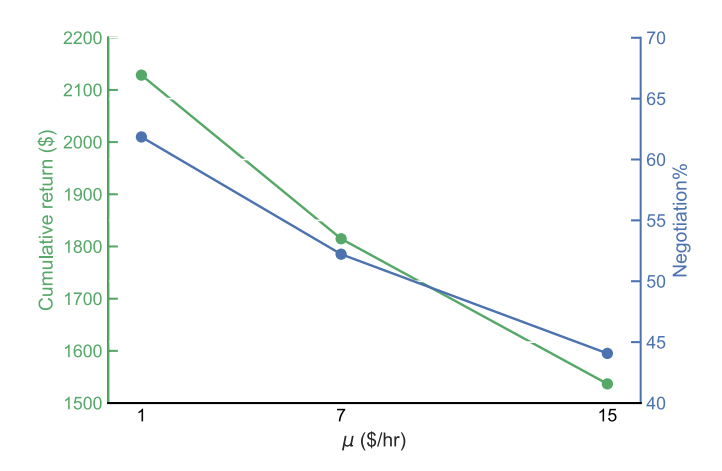


Fig. 14. Impact of  $\mu$  on cumulative returns and percentage for negotiations.

**Table 7** Mean of a few metrics vs.  $\sigma$ .

σ (\$/h)	v (\$/h)	b (min)	vb (\$)	Acceptance Prob. $\phi$	Expected Return (\$)
1.0	17.2	18.6	5.3	0.98	16.1
2.0	19.0	18.0	5.6	0.95	15.5
3.0	20.4	18.0	5.9	0.93	15.0
4.0	21.6	17.1	5.9	0.91	14.7

expected as higher rider VoT implies that the operator must be more selective in schedule negotiations with riders and expect less cumulative returns.

# 5.2.4. Sensitivity analysis of $\sigma$

Given a diverse customer base, an operator may find that the estimated VoT distribution has substantial variability. Therefore, we next analyze the impact of standard deviation  $\sigma$  on the negotiation results using an example instance #64. Fig. 15 shows how a few key metrics vary with  $\sigma$ . Similar to Fig. 11, a breakpoint exists due to two different routes being involved. We find that as  $\sigma$  increases, v and vb increase while the acceptance probability  $\phi$  decreases. A rider's true VoT is getting harder to predict, and so is the rider's response to a schedule deviation; more incentives are required. Then, the expected return drops. The implication for schedule negotiations is that when riders' behaviors are increasingly uncertain, the effectiveness of negotiations diminishes, and the operator must compensate for a rider's private information.

Table 7 further reports the averages of key metrics over all instances. As  $\sigma$  increases, both v and vb increase, while b is relatively stable. The acceptance probability decreases, as well as the expected return. These results suggest that a larger standard deviation of the VoT distribution leads to less favorable outcomes for the operator.

#### 5.2.5. Sensitivity analysis of maximum deviation

This section examines the effect of maximum deviation  $\bar{b}$  on a per-instance basis. The results presented in Table 8 reveal that as  $\bar{b}$  increases, optimal deviation b also increases while v remains constant, which, in turn, causes a corresponding increase in the vb value. The acceptance probability,  $\phi$ , stays constant regardless of the value of  $\bar{b}$  because v remains unchanged. The expected return also shows a gradual increase with  $\bar{b}$ , although the growth rate diminishes as  $\bar{b}$  increases. This suggests that the operator's payoff improves only moderately when  $\bar{b}$  is sufficiently large. Any further increases in  $\bar{b}$  lead to negligible payoff gains due to the diminishing effect, as shown in Fig. 16. A policy suggestion based on the analysis of field data in the D.C. area is that the maximum duration can be set within the range of 30 min to 45 min.

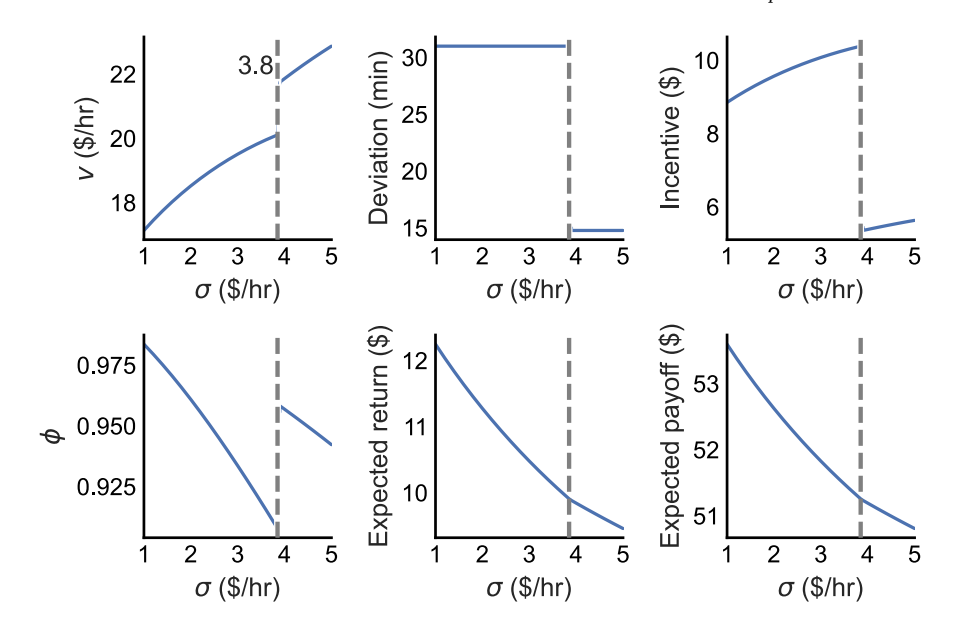


Fig. 15. Impacts of  $\sigma$  on negotiation results.

**Table 8** Mean of a few metrics vs.  $\bar{b}$ .

b (min)	vb (\$)	Acceptance Prob. $\phi$	Expected Return (\$)
7.7	2.4	0.93	10.2
12.7	3.9	0.93	12.0
15.0	4.6	0.93	12.8
16.0	4.9	0.93	12.9
	7.7 12.7 15.0	7.7 2.4 12.7 3.9 15.0 4.6	7.7 2.4 0.93 12.7 3.9 0.93 15.0 4.6 0.93

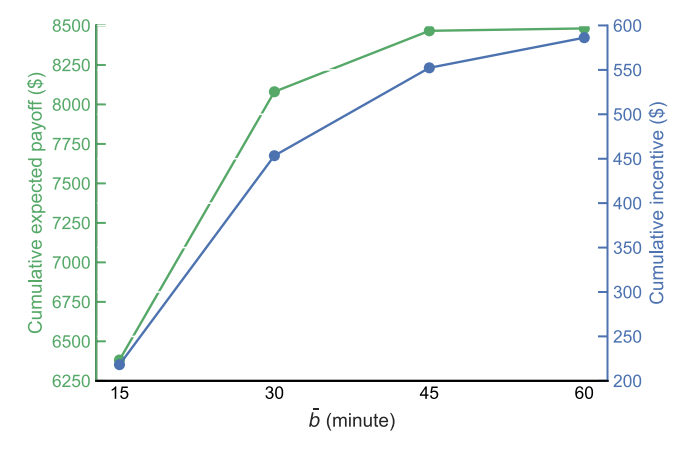


Fig. 16. Impact of  $\bar{b}$  on cumulative expected payoffs and cumulative incentives.

# 6. Conclusions

# 6.1. Summary of main findings

We presented the first known optimization approach for an ADA paratransit operator to conduct pickup time negotiations with its riders at the time of reservation, although schedule negotiation is allowed by the regulations and widely implemented in an *ad hoc* manner. As the operator is unlikely to obtain the private information held by a rider, we explicitly accounted for the probabilistic behavior response of a rider, which differed from the paratransit literature under the complete information assumption. It is important to recognize that even with a substantial amount of data on a rider's past choices, accurately discerning their true preferences remains a near-impossible task for an operator. At best, operators might approximate the true value closely by using the

sample mean. This inherent uncertainty in predicting a rider's choices remains while the degree of uncertainty is limited. Therefore, this study has enhanced rider behavior modeling realism in the paratransit optimization literature.

The proposed negotiable booking confirmation problem is a nonconvex mixed integer nonlinear program, which off-the-shelf optimization solvers cannot solve. Therefore, after analyzing the structural properties of the N-BCP, we presented a few propositions and proposed a fix-and-optimize solution approach after decomposing the solution space. When discrete variables are fixed, the resulting convex optimization problem can be solved optimally. While fixed values of discrete variables can be examined exhaustively, many can be eliminated with the proposed techniques to reduce computation time. The advantage of the proposed fix-and-optimize approach lies in its assurance of global optimum for both discrete and continuous decision variables.

The optimization method has been tested on both synthetic and real-world instances. Among other findings, we highlight the following:

- 1. In the synthetic negotiation instances, the average ROI achieved per instance was 3.5, which means that on the per-negotiation basis, one dollar of incentive leads to a payoff improvement of 3.5 dollars. This clearly demonstrates the high effectiveness of negotiating pickup times in improving paratransit operational efficiency.
- 2. Information about future rider requests, once available, can potentially improve the effectiveness of schedule negotiations over time by avoiding shortsighted decisions.
- 3. Numerical experiments confirmed that the proposed solution approach can ensure solution optimality while requiring substantially less computation time than a benchmark algorithm (a brute force algorithm).
- 4. In real-world case studies, the proposed negotiation mechanism outperformed a benchmark negotiation policy that neglected a rider's value of time uncertainty.

The conducted sensitivity analyses based on real-world data will help paratransit operators understand the relations between the effectiveness of schedule negotiation and key policy parameters, such as the maximum allowable schedule deviation. The state-of-the-practice of schedule negotiation in ADA paratransit is expected to advance consequentially.

#### 6.2. Future work

There are several potential extensions to the current work:

- Multiple Rider Interactions: The immediate extension to the current work would involve examining the interrelations among multiple riders during negotiations. In the current model, negotiations are conducted independently for each incoming rider. Introducing simultaneous negotiations with multiple riders presents greater challenges. The acceptance of one rider might be contingent on the reactions of other riders to the operator's proposed travel plan. In such scenarios, merely maximizing the expected payoff for the operator might not suffice. It might be essential to incorporate risk measurements into decision-making (Sun and Schonfeld, 2016), given the inherent randomness and variability of the optimization objective.
- Machine Learning for Rider Preferences: If there are historical data available regarding a rider's past choices, operators could utilize machine learning to predict the likelihood that a rider will accept a proposed schedule change. This can also provide insights into other rider preferences which might otherwise remain unknown to the operator.
- Accommodating Additional Variability: Another area worth exploring is accommodating both varying drop-off points and schedules for riders when possible.

Furthermore, the modeling framework proposed here has potential applications beyond ADA paratransit. For instance, it could be adapted for decision-making coordination problems in contexts such as peer-to-peer dynamic ridesharing (Sun et al., 2020) and carpooling (Sun et al., 2022).

#### **CRediT** authorship contribution statement

Shijie Chen: Conceptualization, Methodology, Visualization, Writing – original draft. Md Hishamur Rahman: Data curation, Investigation. Nikola Marković: Formal analysis, Investigation, Writing – original draft. Muhammad Imran Younus Siddiqui: Resources, Validation. Matthew Mohebbi: Resources, Validation. Yanshuo Sun: Conceptualization, Methodology, Supervision, Writing – original draft, Writing – review & editing.

# Data availability

Data will be made available on request.

# Acknowledgments

Comments from anonymous reviewers and editors have led to significant improvements to this paper. The authors are grateful for this assistance. The presented research is partially supported by the National Science Foundation, United States (Grant No. 2055347).

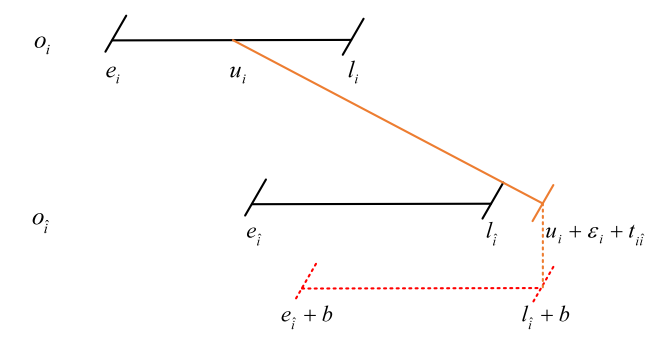


Fig. A.1. New routing feasibility enabled by schedule negotiations.

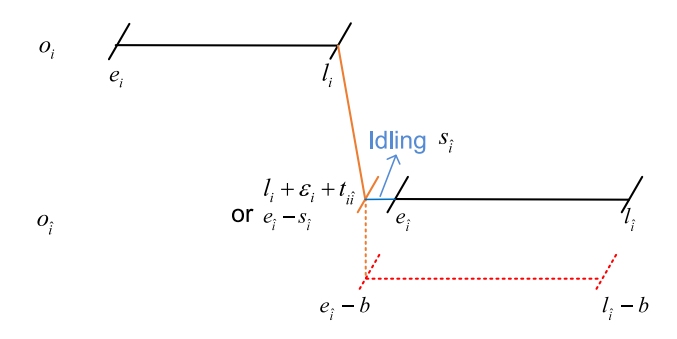


Fig. A.2. Idle time reduction enabled by schedule negotiations.

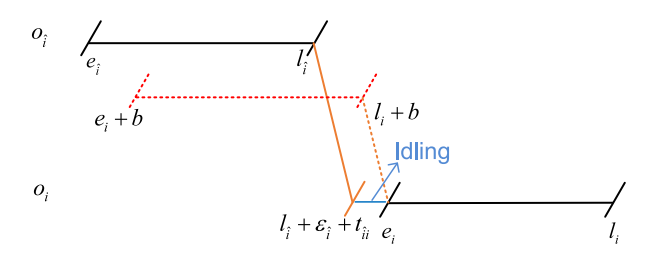


Fig. A.3. Other idle time reductions enabled by schedule negotiations.

#### Appendix. Sources of schedule negotiation benefits

Schedule deviations are expected to improve the cost efficiency of ADA paratransit operations, while the exact sources of these benefits have not been analyzed. Here, we identify three scenarios where a deviated pickup time window would directly yield cost reductions, and thus efficiency gains.

**Enabling additional feasible insertions.** Fig. A.1 shows how it is feasible to visit the new pickup location  $o_i$  immediately after picking up a confirmed rider i at location  $o_i$ , when the pickup time window of new rider  $\hat{i}$  is shifted to the right by b. In this example, the earliest arrival time at location  $o_i$  is  $u_i$  because of other constraints. Even if the vehicle departs immediately after picking up rider i, its arrival time at location  $o_i$  is  $u_i + e_i + t_{i\hat{i}}$ , which violates the pickup time window  $[e_{\hat{i}}, t_{\hat{i}}]$ , unless the window is deviated. The enabled pickup sequence  $o_i \rightarrow o_{\hat{i}}$  may result in an efficient route, which is possible only after the proposed time window  $[e_{\hat{i}} + b, l_{\hat{i}} + b]$  is accepted.

Idle time reduction at new pickup location. Schedule deviations can reduce or eliminate vehicle idling at a new pickup location. Fig. A.2 shows that after picking up a confirmed rider i at the right time window, namely  $l_i$ , the vehicle's arrival time at location  $o_i$  is  $u_i + \epsilon_i + t_{i\hat{i}}$ , which is earlier than the left time window at location  $o_{\hat{i}}$ . In this case, the vehicle idles until new rider  $\hat{i}$  is available at  $e_{\hat{i}}$ . If the new rider's pickup time window is shifted earlier by the same amount as the idling time, namely  $b = s_{\hat{i}}$ , the total cost decreases and payoff increases, because idling a vehicle is much more costly than compensating a rider for schedule deviations, i.e.,  $v < \beta_3$ . More relevant analyses are available in Section 4.1.

**Idle time reduction at other locations.** This case is similar to the second case, and the only difference is that the new rider is picked up before a confirmed rider. Fig. A.3 shows that even though the new rider  $\hat{i}$  is picked up as late as possible, the necessary

idle time  $s_i$  remains when picking up a confirmed rider i. Negotiating a delayed pickup time with rider  $\hat{i}$  can mitigate vehicle idling at location  $o_i$ .

#### References

Agatz, N., Campbell, A., Fleischmann, M., Savelsbergh, M., 2011. Time slot management in attended home delivery. Transp. Sci. 45 (3), 435-449.

Azadeh, S.S., Atasoy, B., Ben-Akiva, M.E., Bierlaire, M., Maknoon, M., 2022. Choice-driven dial-a-ride problem for demand responsive mobility service. Transp. Res. B 161, 128–149.

Berbeglia, G., Cordeau, J.-F., Laporte, G., 2012. A hybrid Tabu search and constraint programming algorithm for the dynamic dial-a-ride problem. INFORMS J. Comput. 24 (3), 343–355.

Bertsimas, D., Jaillet, P., Martin, S., 2019. Online vehicle routing: The edge of optimization in large-scale applications. Oper. Res. 67 (1), 143-162.

Bongiovanni, C., Kaspi, M., Geroliminis, N., 2019. The electric autonomous dial-a-ride problem. Transp. Res. B 122, 436-456.

Braekers, K., Caris, A., Janssens, G.K., 2014. Exact and meta-heuristic approach for a general heterogeneous dial-a-ride problem with multiple depots. Transp. Res. B 67. 166–186.

Coslovich, L., Pesenti, R., Ukovich, W., 2006. A two-phase insertion technique of unexpected customers for a dynamic dial-a-ride problem. European J. Oper. Res. 175 (3), 1605–1615.

Diana, M., Dessouky, M.M., 2004. A new regret insertion heuristic for solving large-scale dial-a-ride problems with time windows. Transp. Res. B 38 (6), 539–557. Dong, X., Chow, J.Y., Waller, S.T., Rey, D., 2022. A chance-constrained dial-a-ride problem with utility-maximising demand and multiple pricing structures.

Transp. Res. E 158, 102601.

Ehmke, J.F., Campbell, A.M., 2014. Customer acceptance mechanisms for home deliveries in metropolitan areas. European J. Oper. Res. 233 (1), 193-207.

Fleckenstein, D., Klein, R., Steinhardt, C., 2023. Recent advances in integrating demand management and vehicle routing: A methodological review. European J. Oper. Res. 306 (2), 499–518.

FTA, 2020. Americans with disabilities act: Guidance. https://www.transit.dot.gov/regulations-and-guidance/fta-circulars/americans-disabilities-act-guidance-pdf. [Online; Accessed 01 March 2023].

Ho, S.C., Szeto, W.Y., Kuo, Y.-H., Leung, J.M., Petering, M., Tou, T.W., 2018. A survey of dial-a-ride problems: Literature review and recent developments. Transp. Res. B 111, 395–421.

Jaw, J.-J., Odoni, A.R., Psaraftis, H.N., Wilson, N.H., 1986. A heuristic algorithm for the multi-vehicle advance request dial-a-ride problem with time windows. Transp. Res. B 20 (3), 243–257.

Klein, R., Neugebauer, M., Ratkovitch, D., Steinhardt, C., 2019. Differentiated time slot pricing under routing considerations in attended home delivery. Transp. Sci. 53 (1), 236–255.

Luo, Z., Liu, M., Lim, A., 2019. A two-phase branch-and-price-and-cut for a dial-a-ride problem in patient transportation. Transp. Sci. 53 (1), 113-130.

Mackert, J., 2019. Choice-based dynamic time slot management in attended home delivery. Comput. Ind. Eng. 129, 333-345.

Masmoudi, M.A., Hosny, M., Braekers, K., Dammak, A., 2016. Three effective metaheuristics to solve the multi-depot multi-trip heterogeneous dial-a-ride problem. Transp. Res. E 96, 60–80.

McGill, J.I., Van Ryzin, G.J., 1999. Revenue management: Research overview and prospects. Transp. Sci. 33 (2), 233-256.

Miami-Dade County, 2015. Special transportation service (STS) rider's guide. https://www.miamidade.gov/transit/library/sts-riders-guide.pdf. [Online; Accessed 01 March 2023].

Molenbruch, Y., Braekers, K., Caris, A., 2017. Typology and literature review for dial-a-ride problems. Ann. Oper. Res. 259 (1), 295-325.

PVTA, 2019. ADA paratransit. https://www.pvta.com/mobility.php. [Online; Accessed 01 March 2023].

Rist, Y., Forbes, M.A., 2021. A new formulation for the dial-a-ride problem. Transp. Sci. 55 (5), 1113-1135.

Strauss, A.K., Klein, R., Steinhardt, C., 2018. A review of choice-based revenue management: Theory and methods. European J. Oper. Res. 271 (2), 375–387. Su, Y., Dupin, N., Puchinger, J., 2023. A deterministic annealing local search for the electric autonomous dial-a-ride problem. European J. Oper. Res. 309 (3), 1091–1111

Sun, Y., Chen, S., Guo, Q., 2022. Evaluating the environmental benefits of personalized travel incentives in dynamic carpooling. KSCE J. Civ. Eng. 1-12.

Sun, Y., Chen, Z.-L., Zhang, L., 2020. Nonprofit peer-to-peer ridesharing optimization. Transp. Res. E 142, 102053.

Sun, Y., Schonfeld, P., 2016. Holding decisions for correlated vehicle arrivals at intermodal freight transfer terminals. Transp. Res. B 90, 218-240.

Vinsensius, A., Wang, Y., Chew, E.P., Lee, L.H., 2020. Dynamic incentive mechanism for delivery slot management in e-commerce attended home delivery. Transp. Sci. 54 (3), 567–587.

Waßmuth, K., Köhler, C., Agatz, N., Fleischmann, M., 2023. Demand management for attended home delivery-A literature review. European J. Oper. Res. 311 (3), 801-815.

Wong, K.-I., Han, A., Yuen, C., 2014. On dynamic demand responsive transport services with degree of dynamism. Transp. A: Transp. Sci. 10 (1), 55-73.

Zhang, D., Adelman, D., 2009. An approximate dynamic programming approach to network revenue management with customer choice. Transp. Sci. 43 (3), 381–394.